Influence of waves on the transport and fate of outfall sediments

Diego. A. Casas[a]*, Tobias Bleninger[a,b], Maurício F. Gobbi[b], Silene C. Baptistelli[c]

[a] Graduate Program of Water Resources and Environmental Engineering (PPGERHA), Federal University of Paraná (UFPR), Curitiba, 81531-980, Paraná, Brazil. ORCID: 0000-0002-3904-2422 (D.A.C.); 0000-0002-8376-3710 (T.B.).

[b] Graduate Program of Environmental Engineering (PPGEA), Federal University of Paraná (UFPR), Curitiba, 81531-980, Paraná, Brazil. ORCID: 0000-0001-9185-5212 (M.F.G.).

[c] Sanitation Company of São Paulo State (Sabesp), São Paulo, 81531-980, São Paulo State, Brazil.

* Corresponding author. E-mail: diego.casas@upfr.br

Abstract

An analysis of the effects of waves on the transport and fate of sediments from submerged outfalls in relatively shallow waters is presented. Five sewage outfalls in the coastal area of Baixada Santista, Brazil, were selected as a case study. A hydrodynamic model both with and without wave effects was implemented, and sediment discharges from the five outfalls were considered. The results from current-only and wave-current models were compared to identify differences in the transport of outfall sediments due to waves. If waves are not considered, the model simulates a continuous deposition that results in unrealistic bed sediment accumulation. Significant wave-induced resuspension was observed near the outfall diffusers, even during mild wave conditions. Under mean and strong waves, the resuspended sediment can be transported further and reach nearby coasts and channels. Overall, results indicate that coupled wave-current models can serve to better understand the fate of sediment-attached pollutants from outfalls.

Keywords: hydrodynamic modeling, marine outfall, sediment resuspension, wave-current interaction.

1. Introduction

Coastal wastewater disposal is often done by means of submerged outfalls. These are pipelines designed to discharge raw or partially treated wastewater to the seabed at a certain distance from the shoreline. At the discharge location, the outfall has a diffuser that facilitates the dilution of the effluent in seawater. The dilution process depends on several factors: wastewater flowrate, water depth, diffuser geometry and oceanic conditions such as currents, stratification, tides and turbulence (Tate, Scaturro, and Cathers 2016). The analysis and modeling of outfall plumes is generally performed considering three regions: near field; mid field; and far field. In the near field, plume dynamics is dominated by the outflow; in the far field, plume behavior is dominated by ocean currents; and the mid field is a transition zone (Morelissen, van der Kaaij, and Bleninger 2013). Most of the dilution occurs in the near field, while in the far field, the plume is mainly transported by ambient currents with a much lower mixing dominated by natural processes (Roberts 1991).

Apart from the effects on water quality, wastewater disposal in coastal waters is known to produce sediment pollution. Sediment pollution can occur when contaminated particles are directly released into a body of water or when suspended or bed sediments absorb water contaminants (Megahan 1999). Contaminated particles may come from domestic, commercial and industrial wastewater. In particular, domestic sewage solids can have different sizes, from fine fecal and other organic particles to large organic matter and sewage litter (Ashley and Hvitved-Jacobsen 2003). In the case of combined drainage systems, raw sewage can contain solids from stormwater runoff as well. Total suspended solids in municipal wastewater are typically less than 0.1% with concentrations of 120 to 400 mg/L (Metcalf & Eddy 2014), but in combined systems they can reach up to 1722 mg/L (Suárez and Puertas 2005).

The seabed in coastal areas receiving wastewater discharges is commonly characterized by a superficial layer of organic mud with black or gray coloration (Wasserman, Freitas-Pinto, and Amouroux 2000; Gkaragkouni et al. 2021). Elevated concentrations of different types of pollutants have been reported in sediment samples in the vicinity of marine outfalls, e.g., heavy metals (Hershelman et al. 1981; Soto-Jiménez, Páez-Osuna, and Morales-Hernández 2001; Gkaragkouni et al. 2021), toxic organic contaminants (Moon et al. 2008; Akdemir and Dalgic 2021) and contaminants of emerging concern such as microplastics (Reed et al. 2018) and pharmaceutical products (Maruya et al. 2012).

Near-field particle deposition from outfalls jets in stagnant and flowing environments have been extensively investigated (M. J. Neves and Fernando 1995; Bleninger and Carmer 2000; Lane-Serff and Moran 2005; Cuthbertson et al. 2008; Terfous, Chiban, and Ghenaim 2016). However, transport and fate of outfall sediments in the far field have not received as much attention although it is phenomenologically understood (e.g., Herring 1980). Simplified methods have been applied to obtain estimates of deposition and resuspension of outfall particulates (Bodeen et al. 1989; Ferré, Sherwood, and Wiberg 2010; Tate, Holden, and Tate 2019). Detailed modeling has been done, e.g., by Hodgins, Hodgins, and Corbett (2000), who implemented a three-dimensional particle deposition model for sewage solids from a large submerged outfall under tidal currents. Still, most modeling efforts focus on analyzing the wastewater plume with little or no detail on the solid fraction of the plume (e.g., Pritchard, Savidge, and Elsäßer 2013; Uchiyama et al. 2014; Falkenberg et al. 2016; Veríssimo and Martins 2016; Roberts and Villegas 2017; Ostoich et al. 2018; Mrša Haber et al. 2020; Birocchi et al. 2021). On the other hand, coastal processes such as internal or surface waves can resuspend the solid particles, which then undergo further transport by currents along the shelf (Lee, Noble, and Xu 2003). In particular, in shallow waters, the combined action of surface waves and currents may generate frequent events of resuspension that can release dissolved metals and nutrients (Kalnejais, Martin, and Bothner 2010). Also, sediment resuspension can act as a bacterial input mechanism for the overlying water column (Gao, Falconer, and Lin 2013).

Although the influence of internal waves on outfall sediment resuspension has been studied before (Tate, Holden, and Tate 2019), surface waves have only been pointed out as a potentially relevant process with no detailed studies on the matter (Wu, Washburn, and Jones 1991; Lee, Noble, and Xu 2003; R. Neves 2006; Bleninger 2006). To the knowledge of the authors, no detailed research has been done on assessing the relative importance of surface waves in far-field modeling of submerged outfalls. Only a few academic studies have included waves into the hydrodynamic modeling of outfalls (Inan 2019; Kim et al. 2021); however, they are neither concerned with assessing the effects of waves nor do they include sediment transport. Given the lack of studies on the relevance of waves in far-field outfall models, their inclusion in academic or engineering studies is almost discretionary. In this regard, the present study aims to make an initial attempt to assess the relative importance of waves and wave-current interactions for far-field modeling of submerged outfalls.

Considering that waves may have significant effects on outfall sediment transport, an ensemble of five submerged outfalls in the metropolitan area of Baixada Santista in São Paulo State, Brazil, was selected as a case study. There is one outfall in the Santos municipality, another in Guarujá and three in Praia Grande (PG1, PG2 and PG3). These outfalls discharge sewage at shallow depths (<15 m) where surface waves may play a significant role in the resuspension of effluent sediment. In Baixada Santista, bed sediment quality is of concern. A recent report by the Environmental Agency of São Paulo State (CETESB 2022), showed elevated concentrations of total organic carbon, Kjeldahl nitrogen, phosphorus and *Clostridium perfringens* bacteria in sediments from the influence area of the PG1 outfall, as well as elevated concentrations of thermotolerant coliforms and *C. perfringens* in sediments near the discharge locations of the Santos and Guarujá outfalls, respectively. Several authors have found high toxicity to benthic amphipods in sediment samples in the vicinity of the Santos outfall diffuser (Abessa et al. 2005; Cesar et al. 2006; Abessa et al. 2008; Sousa et al. 2014; Vacchi et al. 2019). Vacchi et al. (2019) demonstrated that the toxicity is related to organic contaminants absorbed by the sediment particles. Furthermore, recent studies have found high levels of contaminants of emerging concern in sediments in the vicinity of the outfalls discharge locations. For example, endocrine disrupting chemicals for outfalls of Santos, Guarujá, PG1 and PG2 (Santos et al. 2018), and rhodium for Santos (Berbel et al. 2021).

Direct measurements of outfall sediment transport could provide a better understanding of the influence of the outfalls on sediment quality. However, in the absence of direct field measurements, a numerical model can provide major insights on outfall sediment transport. Consequently, the present study is concerned with the transport and fate of sediment from the five submerged outfalls in Baixada Santista from a modeling perspective. Since the outfalls discharge their effluents in relatively shallow waters exposed to the open ocean, the use of a coupled wave-current hydrodynamic model is proposed. The objective of the study is to assess the relative importance of waves and the combined action of waves and currents for far-field modeling of submerged outfall sediments. Hydrodynamic and wave propagation models for the coastal area of Baixada Santista were implemented using the Delft3D modeling suite (Deltares 2020a; 2020b). These models were calibrated and validated using field data such as water level and wave buoy measurements. Sediment transport was implemented only for the outfall effluents, so other sources of sediment were not included, e.g., streams, longshore drift, surface runoff. In order to assess the effects of wave-current interaction on sediment transport and fate, the results of standalone hydrodynamic models were compared with coupled wave-current models for mild, mean and strong wave regimes. The focus was on sediment resuspension events, and special attention was given to wave conditions that produced or enhanced the phenomenon.

2. Materials and Methods

2.1. Site description

Baixada Santista is a metropolitan area located in the coastal region of São Paulo State, Brazil. It comprises nine municipalities and is served by five submerged wastewater outfalls operated by the Sanitation Company of São Paulo State (Sabesp). There is one outfall in the Santos municipality, another in Guarujá and three in Praia Grande (see Figure 1b). The Santos outfall consists of a concrete-covered steel pipe that discharges wastewater from the Santos and São Vicente municipalities into the Santos Bay. Outfalls of Guarujá and Praia Grande discharge directly to the Atlantic Ocean through high-density polyethylene pipes.

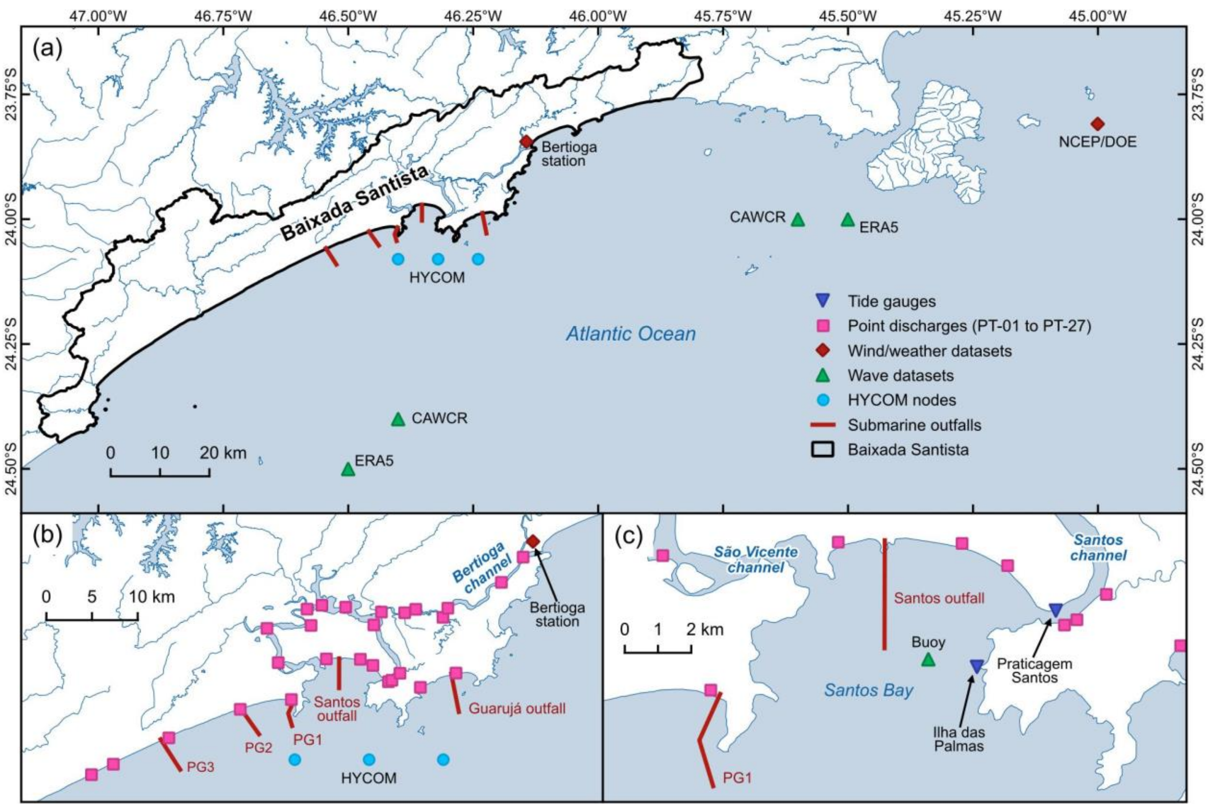

Figure 1: Location of the study area and points of interest.

Until 2019, the effluent of Santos outfall had primary treatment with 1.5 mm screening and disinfection. Up to that year, the effluent of outfalls Guarujá and PG3 also received primary treatment, while effluents of outfalls PG1 and PG2 only received preliminary treatment. As of 2020, several engineering efforts and operational improvements have been made (e.g., primary treatment for all outfalls and outfall length extensions for PG1 and PG2). General characteristics for 2019 of the five outfalls are summarized in Table 1. It is worth noting that for the studied time periods, outfall discharges did not reach the maximum design values.

Table 1: Characteristics of the submerged outfalls in Baixada Santista (data for 2019).

Outfall	Length (m)	Diameter (m)	Depth (m)	Design discharge (m^3/s)	Reynolds number	Densimetric Froude number	Inclination
Santos	4425	1.75	11.5	5.30	3.88×10^5	22.6	Horizontal
Guarujá	4500	0.90	14.0	1.45	9.55×10^4	18.0	Horizontal
PG1	4000	1.00	14.0	1.20	9.55×10^4	18.0	Horizontal
PG2	4000	1.00	14.0	1.20	9.88×10^4	14.1	Horizontal
PG3	4095	1.00	13.0	0.78	2.05×10^5	29.4	Horizontal

Baixada Santista is located on a coastal plain delimited by the Serra do Mar mountain system and the Atlantic Ocean. One of the most prominent morphological features along its shoreline is the Santos estuarine system, which comprises the Santos Bay and the estuarine channels of São Vicente, Bertioga and Santos (Figure 1b,c). Santos Bay is a semi-sheltered and shallow bay (depths between 5 m and 15 m). The study area presents a mainly semidiurnal tide with diurnal inequalities (Schettini et al. 2019). Inside the bay, spring and neap tides have amplitudes of about 0.6 m and 0.14 m, respectively (Harari, França, and Camargo 2008). Also, the region is under the influence of cold fronts about every two weeks (Escobar, Reboita, and Souza 2019) that, each, generate strong winds for nearly two consecutive days (Stech and Lorenzzetti 1992).

Tides are of great importance for eddy diffusivity and vertical mixing inside Santos Bay. Salinity measurements during neap and spring tides show that the estuary is weakly stratified near its head and at the entrance of the channels (Harari, França, and Camargo 2008). Other studies have found that Santos Bay and its outer coastal area are well mixed during spring tides (Belém et al. 2007). Furthermore, suspended solids concentrations are of the order of 10^{-2} kg/m^3 and can be considered horizontally and vertically homogeneous in most of the bay, showing no significant influence of spring and neap tides (Berzin 1992).

Most of the year, waves approach the continental shelf from south, with heights of 1 m to 3 m and periods of 10 s to 12 s, and the highest waves usually come from the southwest, reaching up to 6.3 m (Pianca, Mazzini, and Siegle 2010). The dominant waves get refracted toward Baixada Santista, arriving rather from the southeast as seen in the wave rose plot of Figure 2. As it is typical in the southern and southeastern Brazilian coast, the region is characterized by multi-modal sea states consisting of a locally generated wind wave system and two or more swells propagating from distant fetches (Violante-Carvalho et al. 2001; Innocentini, Caetano, and Carvalho 2014). This is also suggested by the unalignment between wind and wave roses in Figure 2. The most energetic waves in the region are associated with cold fronts and have a significant impact on the local morphodynamics (Stein and Siegle 2019).

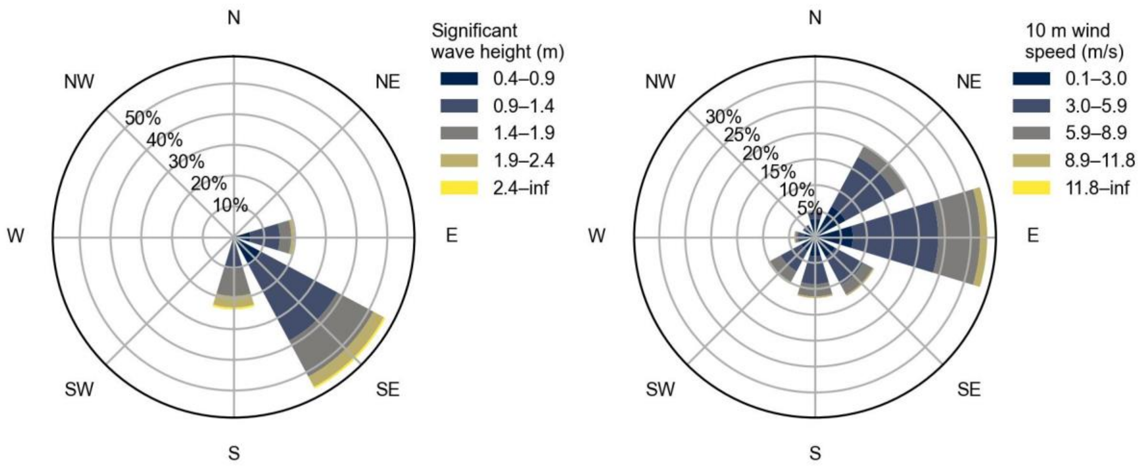

Figure 2: Wave rose from the western CAWCR node (24.4°S, 46.4°W) and wind rose from its respective ERA5 node.

2.2. Available data

Topographic and bathymetric data of Baixada Santista were obtained from different sources such as bathymetric surveys performed by the Santos Pilotage Service (Praticagem do Porto de Santos); nautical charts from the Brazilian Navy's Directorate of Hydrography and Navigation (DHN); the General Bathymetric Chart of the Oceans (GEBCO); the SRTM15+V2.0 global elevation grid (Tozer et al. 2019); and sparse survey data provided by Sabesp.

Water level time series from tide gauges of Praticagem Santos and Ilha das Palmas were provided by DHN. Both tide gauges are located inside the Santos estuary. The former is at the entrance of the Santos channel; the latter is on an island to the east of Santos Bay. Marine climate data such as water temperature, salinity, and currents, were retrieved from nodes of the Hybrid Coordinate Ocean Model (HYCOM; Bleck 2002). Observational data of wind velocity and direction were available at the Bertioga station owned by the Brazilian National Institute of Meteorology (INMET). However, auxiliary wind fields were retrieved from an atmospheric reanalysis of the United States National Centers for Environmental Prediction (NCEP) (NCEP/DOE Reanalysis 2; Kanamitsu et al. 2002). Other required meteorological variables such as relative humidity, air temperature and net solar radiation were also extracted from the NCEP/DOE Reanalysis. Figure 1 shows the location of the tide gauges, the meteorological station and the HYCOM and NCEP/DOE global grid nodes employed in the study.

Data on outfall discharges for 2012 and 2019, as well as sparse analyses of total suspended solids of their effluents for 2019, were provided by Sabesp (2023). The outfall discharge time series were analyzed for inconsistencies on a monthly basis, replacing suspicious records with compatible records from the previous or following year. The consolidated discharge time series are shown in Figure A1 of the Appendix. Additionally, from an analysis of the drainage system of Baixada Santista, there were identified a total of 27 freshwater point discharges (PT-01 to PT-27) into the coastal area influenced by the five submerged outfalls (see Figure 1b,c). The point discharges correspond to streams and other effluents with mean annual flows between 0.15 m^3/s and 25.26 m^3/s (see Table A1 in Appendix).

Regarding the wave climate, time series of significant wave height at a buoy in Santos Bay (see Figure 1c) were provided by Fundação Centro Tecnológico de Hidráulica (FCTH). Hourly-averaged wave parameters in deep water were obtained from the European Centre for Medium Range Weather Forecasts (ECMWF) fifth generation reanalysis (ERA5; Hersbach et al. 2020) and the Collaboration for Australian Weather and Climate Research (CAWCR) wave hindcast (Smith et al. 2021). The ERA5 and CAWCR grid nodes employed for the study are shown in Figure 1a. Since wind fields are an important input for wave propagation models, three global wind datasets were considered. In addition to ERA5 which also provides wind data (recall Figure 2), we used wind fields from the United States National Aeronautics and Space Administration (NASA) Modern-Era Retrospective Analysis for Research and Applications, version 2 (MERRA-2; Gelaro et al. 2017) and the NCEP Climate Forecast System, version 2 (CFSv2; Saha et al. 2014). These wind datasets provide data on global grids with size between 0.2° and 0.625°, and hourly temporal resolution.

2.3. Hydrodynamic model

The hydrodynamic and sediment transport modeling was performed with the Delft3D-FLOW module. Delft3D-FLOW simulates two-dimensional or three-dimensional hydrodynamic flows and transport phenomena over a domain driven by environmental forces. This module solves the unsteady non-linear shallow water equations under hydrostatic and Boussinesq approximations (Deltares 2020a). Delft3D-FLOW is widely employed in studies regarding coastal and estuarine environments (Baptistelli 2015; Mendes et al. 2021; Huff, Feagin, and Figlus 2022), and it has been validated by laboratory and field studies (Elias et al. 2001; Gerritsen et al. 2008).

Two simulation periods, i.e., 2012 and 2019, were considered for the Delft3D-FLOW model. Calibration and validation of hydrodynamics were done for 2012 because of tide gauge data availability. However, the period employed for outfall sediment transport modeling was 2019 since suspended solid concentrations of the outfall effluents were only known for that year.

The computational domain was prescribed as a two-dimensional structured curvilinear grid with variable spatial resolution between 36 m and 1014 m. Variable resolution allows for a more detailed simulation in areas of interest while not consuming excessive computer power in other areas, e.g., near the boundaries. A mesh sensitivity analysis was done by refining in the areas of interest (the vicinity of the outfalls and the Santos Bay), and the model was found to have negligible mesh dependency for cell sizes of the order of 100 m near the outfall discharge locations. In Delft3D-FLOW, a two-dimensional grid implies a depth-average simulation, which is justified in the present study because Santos Bay and its outer coastal area are weakly and briefly stratified during both neap and spring tide regimes (Belém et al. 2007; Harari, França, and Camargo 2008). Bed elevations for this grid were interpolated from the available topographic and bathymetric datasets. Figure 3 shows the grid definition and interpolated bathymetry.

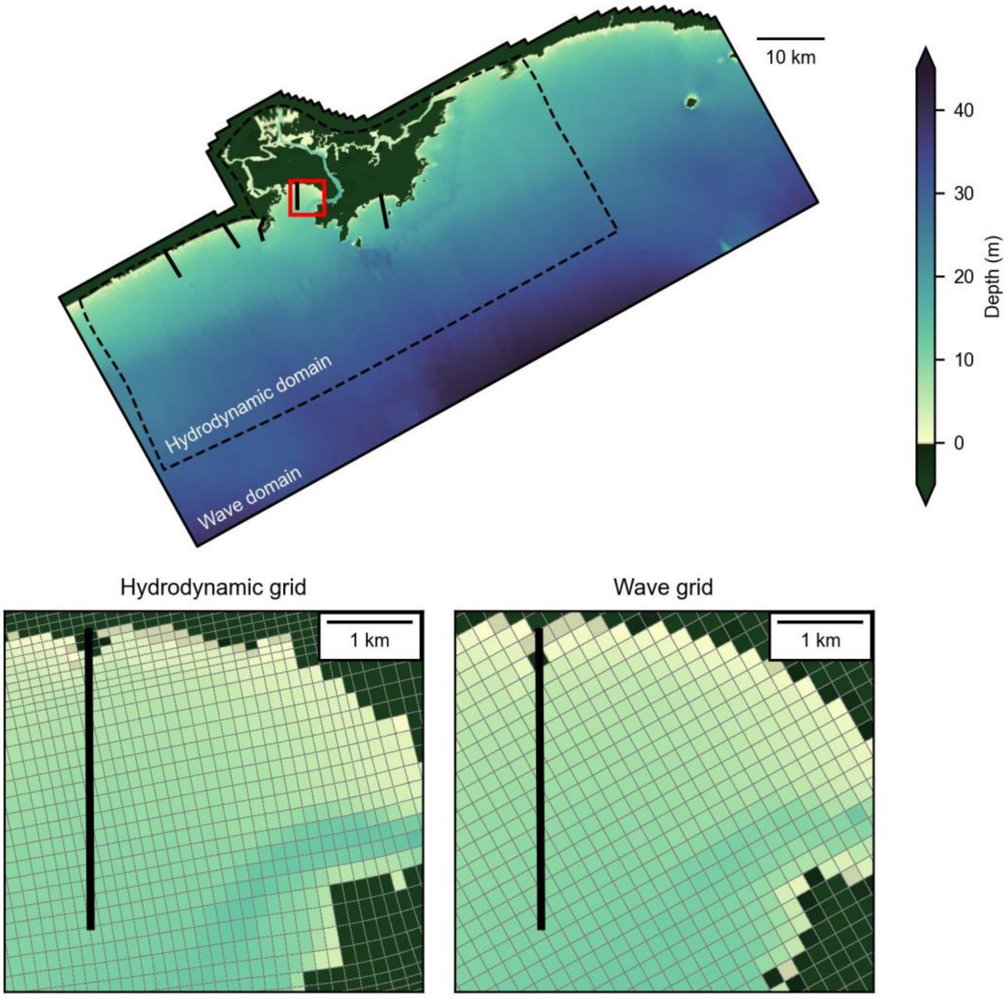

Figure 3: Computational grids with interpolated bathymetry.

Water level boundary conditions in open ocean were specified via amplitudes and phases of 14 tidal constituents from the TPXO global tidal model (Egbert and Erofeeva 2002). These harmonic constants were downloaded and spatially interpolated along western, southern and eastern boundaries using Delft Dashboard (Ormondt, Nederhoff, and Dongeren 2020). Time-varying salinity and temperature conditions from HYCOM were also specified at open boundaries for 2012 and 2019.

Uniform wind forcing was applied for the model by providing time series of wind speed and direction at 10 m elevation. For the 2012 period, wind time series from Bertioga station presented significant gaps, so NCEP/DOE winds were utilized. For 2019, Bertioga station was used since it presented robust time series with hourly resolution, whereas NCEP winds were 6-

hourly. Sensitivity analyses on available subperiods showed that both wind datasets produce similar hydrodynamic results, so the most complete dataset was selected for each period.

For modeling heat exchange at the free surface, the Murakami scheme (Murakami, Oonishi, and Kunishi 1985) was used. This heat flux model considers the absorption of incoming radiation as a function of depth, and, although developed for Japanese waters, it has been applied to coastal waters in other regions (e.g., Pokavanich, Nadaoka, and Blanco 2008; Alosairi, Pokavanich, and Alsulaiman 2018; Arifin, Yano, and Lando 2020). Time series of uniform relative humidity, air temperature and net solar radiation from the NCEP/DOE Reanalysis were prescribed for the Murakami scheme in both 2012 and 2019.

Constant flows were prescribed for the 27 point discharges corresponding to their mean annual flows in 2012 and 2019 (Table A1). Outfall discharges were prescribed as monthly averages in a single grid cell according to available data for both simulation periods. The mean monthly discharges of each outfall for 2012 and 2019 were defined as shown in Figure A1. Constant salinity of 0.1 ppt and temperature of 20°C were set for all freshwater point discharges and outfalls.

Model calibration was done mainly by minimizing the difference in water level between model results and measurements at Praticagem Santos for 2012. Differences in currents, salinity and temperature between the model and the HYCOM node near Praia Grande were also considered. The calibrated model was validated against water level time series at Ilha das Palmas for 2012 and compared with currents, salinity and temperature time series at the HYCOM nodes near Santos and Guarujá. Major calibration parameters were the Manning's bottom roughness coefficient, the wind drag coefficient and the time step. Calibration was achieved with a Manning's coefficient of 0.02 and a linear wind drag coefficient between 0.001 and 0.003 for wind speeds between 0 m/s and 25 m/s. The simulation time step was defined to be 1 minute.

In depth-averaged models, Delft3D-FLOW implements constant values for horizontal eddy viscosity and diffusivity to account for momentum and solute mixing due to unresolved turbulent motion (Deltares 2020a). Since the vertical profile of the horizontal velocity is not resolved, these viscosity and diffusivity parameters must also account for shear dispersion. The eddy viscosity and diffusivity are usually calibration parameters since they are flow-dependent properties, in contrast to their molecular counterparts, which are properties of the fluid. Given the lack of measurements of velocity and solute dispersion in the study area, calibration for those parameters was not possible. However, preliminary simulations were performed to study the sensitivity of the model to background eddy viscosity and diffusivity in a range of 10^{-2} m^2/s and 10^2 m^2/s. Variations in viscosity and diffusivity did not have significant effects on the order of magnitude of suspended sediment concentration and deposition rate. Water level and velocity inside the Santos Bay also showed low sensitivity to variations in eddy viscosity and diffusivity. Then, it is reasonable to assume that uncertainties in unresolved flow features (i.e., turbulence and shear dispersion) do not phenomenologically invalidate the conclusions of the present research. Finally, both background horizontal eddy viscosity and diffusivity were set to a uniform value of 1 m^2/s.

Finally, the case setup for periods 2012 and 2019 are consolidated in Table 2 with the main model inputs and the available data for each parameter/forcing.

Table 2: Summary of hydrodynamic model inputs.

Input	2012	2019
Manning coefficient	0.02	0.02
Horizontal eddy viscosity	1 m^2/s	1 m^2/s
Horizontal eddy diffusivity	1 m^2/s	1 m^2/s
Boundary conditions		
Water level	TPXO	TPXO
Temperature and salinity	HYCOM	HYCOM
Wind speed and direction	NCEP/DOE	Bertioga station
Surface heat flux		
Model	Murakami	Murakami
Relative humidity	NCEP/DOE	NCEP/DOE
Air temperature	NCEP/DOE	NCEP/DOE
Net solar radiation	NCEP/DOE	NCEP/DOE
Outfall discharges		
Flow	Figure A1	Figure A1
Temperature	20°C	20°C
Salinity	0.1 ppt	0.1 ppt
PT-01 to PT-27 discharges		
Flow	Table A1	Table A1
Temperature	20°C	20°C
Salinity	0.1 ppt	0.1 ppt
Sediment transport	No	Yes

2.4. Sediment transport modeling

The suspended sediment concentrations in outfall discharges were estimated from analyses of total suspended solids of the outfall effluents in 2019. Constant total sediment concentrations were estimated to be 0.278 kg/m^3 for Santos outfall, 0.128 kg/m^3 for Guarujá outfall and 0.134 kg/m^3 for the three outfalls at Praia Grande. The grain size distribution was determined by laser diffraction granulometry of solids of a wastewater sample from the Santos treatment plant in March 2016 (Consórcio Partner/TetraTech 2017). The median grain size of the whole sample was 20 μm, showing that the effluent solids are mainly silt-sized. Given that the minimum median grain diameter accepted by Delft3D for non-cohesive sediment is 100 μm, the total suspended solids were divided into cohesive and non-cohesive fractions (see Figure A2 in Appendix). For the non-cohesive fraction, the median size of 100 μm was found in the upper 18% of the grain size distribution (>62.4 μm) The lower 82% is then considered as cohesive sediment with a median size of 14.7 μm. The concentrations of suspended solids were split accordingly for each outfall.

By default, Delft3D uses a particle density of 2650 kg/m^3, typical of mineral sediments. However, since wastewater effluents usually contain a significant fraction of lighter organic particles (1250 kg/m3 on average; Boyd 1995), the default specific density must be corrected. Laboratory analysis of wastewater samples from the Santos treatment plant in 2015 (Figure A2 in Appendix) shows that on average suspended solids are 81% volatile (organic) and 19% fixed (mineral). Following Avnimelech et al. (2001) and considering the organic and mineral content, a weighted average specific density of 1513 kg/m^3 was computed. Since dry bed density of the effluent solids was not available, it was estimated from the weighted specific density and the default porosity considered by Delft3D (81% and 40% for cohesive and non-cohesive sediments, respectively). Then, the bed dry densities were specified as 286 kg/m^3 for the cohesive fraction and 914 kg/m^3 for the non-cohesive fraction. Sediment dynamics of cohesive sediment depends on several other factors such as the settling velocity, salinity-induced sediment flocculation and empirical parameters for sedimentation and erosion. However, these parameters were not available for the present study, so Delft3D defaults were used.

In order to analyze the transport and fate of sediment exclusively from the outfalls, initial sediment concentration and bed sediment layer were set to zero, and all other sources of sediment were disabled (i.e., concentration in point discharges and boundaries equal to zero). The overall setup of the sediment transport model is summarized in Table 3.

Table 3: Summary of sediment transport inputs.

Input	Cohesive (82%)	Non-cohesive (18%)	Total sediments
Median grain size (μm)	14.7	100	20
Specific density (kg/m^3)	1513	1513	1513
Initial bed layer thickness (m)	0	0	0
Concentration (kg/m^3)			
Initial	0	0	0
Santos	0.228	0.050	0.278
Guarujá	0.105	0.023	0.128
PG1, PG2 and PG3	0.110	0.024	0.134
PT-01 to PT-27	0	0	0

2.5. Wave model

In order to simulate the propagation and evolution of wind-waves in the domain, the Delft3D-WAVE module was used. Delft3D-WAVE computes wave fields for given bathymetry, wind field and hydrodynamic conditions by running the SWAN model (Deltares 2020b). SWAN is a third-generation wave model that simulates the generation and propagation of wind-waves in coastal regions including shallow waters and ambient currents (Booij, Ris, and Holthuijsen 1999). SWAN is widely used for studies of waves in coastal environments, estuaries, tidal inlets and semi-enclosed basins (e.g., Lenstra et al. 2019; Rusu 2022; Iouzzi et al. 2022; Aydoğan and Ayat 2021), and it has been validated for a number of field and academic cases (Ris, Holthuijsen, and Booij 1999; Allard et al. 2004).

For wave modeling, two periods were considered. The period for validation was 2016 due to availability of wave data from the buoy in Santos Bay. To study the influence of waves on outfall sediment transport, the period of 2019 was set up for wave-current coupling.

The wave domain was discretized as a structured grid with uniform resolution of 205 m and oriented along the hydrodynamic grid. A mesh sensitivity analysis starting with grid size of 409 m with gradual reductions showed that the model was approximately mesh independent at 205 m. Further refinement caused the greatest wave height improvement to be less than 2 cm at the cost of much longer computation times. In the same fashion as for the hydrodynamic model, bathymetry was interpolated from available surveys and datasets. The computational grid of the wave model was defined to be larger than the hydrodynamic grid (see Figure 3) to simulate wave propagation from global hindcast nodes in deep waters (ERA5 and CAWCR). In practice, when a coupled simulation is performed, hydrodynamic and wave grids do not need to be identical since Delft3D can interpolate the required wave output to the hydrodynamic grid and vice-versa.

In the present simulation, the following processes were considered: energy input by wind; dissipation by bottom friction, depth-induced breaking and whitecapping; and non-linear wave-wave interactions, i.e., quadruplets and triads. For bottom friction, Delft3D-WAVE applies by default the empirical JONSWAP formulation (Hasselmann et al. 1973) with a bottom friction coefficient of 0.067 m^2/s^3, as proposed by Bouws and Komen (1983) for fully developed wind-sea conditions in shallow water. However, a more recent study by Vledder, Zijlema, and Holthuijsen (2011) shows that the value 0.038 m^2/s^3 is applicable for a wide range of bottom materials and for both wind-sea and swell, so it is used in the present simulation.

For model input, space-varying and time-varying eastward and northward 10 m wind speed components were defined as subsets of the global atmospheric reanalyses over the sea surface, i.e., ERA5, CFSv2 and MERRA-2. Following the default JONSWAP boundary condition parametrization in SWAN, time series of significant wave height, peak period, mean wave direction and directional spreading were generated from global wave datasets (ERA5 and CAWCR). In the present model, SWAN performs spectral interpolation between two support points to establish boundary conditions for all grid points along the southern boundary.

The selection of appropriate wind field and wave boundary conditions was conducted by cross validation, i.e., testing a total of six different combinations of wind and wave datasets and comparing model results with significant wave height time series from a buoy in Santos Bay. The wind datasets considered were ERA5, CFSv2 and MERRA-2, while the wave datasets were from ERA5 and CAWCR. The best wave boundary condition and wind dataset were from CAWCR and ERA5, respectively. This combination is consistent with results from other authors. For example, a study by Kaiser et al. (2022) showed that ERA5 winds produce better results than CFSR for spectral wave modeling in the South Atlantic Ocean. Furthermore, the combination of CAWCR wave boundary conditions with ERA5 wind have been found to provide slightly more accurate results for wave modeling in the southern Brazil nearshore (Bose et al. 2022). The combination of ERA5 winds with CAWCR wave boundary conditions was then used for the 2019 wave-current coupling.

Although the model was set up with input data for the entire year 2019, for convenience, the model runs were performed by sub-periods. According to the time scale of variations in the incoming wave conditions (CAWCR Wave Hindcast), the length for the sub-periods was specified to be a month. The time series of wave integral parameters of 2019 from a CAWCR node were analyzed to determine relevant modeling sub-periods. January, March and July of 2019 were selected being representative of mild, mean and strong wave regimes, respectively. This selection is consistent with regional wave climate, i.e., the austral summer (January) and winter (July) have the higher and lower wave heights (see Pianca, Mazzini, and Siegle 2010). The time series of significant wave height from the westernmost CAWCR node in Figure 1 (24.4°S, 46.4°W) is presented in Figure A3 of the Appendix for the three selected sub-periods.

2.6. Wave-current interaction modeling

The effect of wave-current interaction on the transport and fate of outfall sediment was evaluated by comparing the results of the standalone hydrodynamic model with the coupled hydrodynamic-wave model for the three defined sub-periods. Coupling between Delft3D-FLOW and Delft3D-WAVE was done in online/dynamic mode. This mode allows for a two-way wave-current interaction in which both the effect of waves on currents and the effect of currents on waves are accounted for. Delft3D-FLOW accounts for several wave-induced effects on hydrodynamics. Wave-induced forcing, Stokes drift and the enhancement of bed shear stress by waves have an overall effect over the water column and can be considered in a depth-averaged form suitable for 2D computations (Deltares 2020a).

In particular, the enhancement of bed shear stress by waves results from a non-linear interaction between the bed boundary layers of waves and currents, causing the resultant bed shear stress to be higher than the simple addition of the shear stresses due to waves and currents

(Soulsby and Humphery 1990). The non-linear boundary layer interaction results in time-averaged and maximum components of oscillatory bed shear stress that are important drivers for sediment transport (Deltares 2020a). Sediment resuspension is dominated by the maximum bed shear stress, while overall current velocity and diffusion of suspended particles are influenced by the time-averaged bed shear stress.

3. Results and discussion

3.1. Calibration and validation

The performance of hydrodynamic and wave models was evaluated using error metrics comparing observed and modeled values. Given a series of n observed values, O_i, and their corresponding modeled values, M_i, their means are denoted by $\bar{O}$ and $\bar{M}$, and their sample standard deviations by s_O and s_M. The error metrics are those suggested by Pontius (2022), but the regression slope is from a standardized major axis regression to account for an unknown level of uncertainty in both observations and model results (Correndo et al. 2021). Their definitions and units are given in Table 4.

Table 4: Definition of the proposed error metrics.

Metric	Formula	Units
Mean error (ME)	$\bar{M} - \bar{O}$	From O_i, M_i
Mean absolute error (MAE)	$\frac{1}{n}\sum_{i=1}^{n}\lvert M_i - O_i\rvert$	From O_i, M_i
Pearson correlation coefficient (PCC)	$\frac{\sum_{i=1}^{n} O_i M_i - n\bar{O}\bar{M}}{(n-1)s_O s_M}$	Dimensionless
Regression slope	$\frac{s_M}{s_O}$	Dimensionless

Since the hydrodynamic model was set up for mean conditions, i.e., astronomical tides, the modeled water level does not reflect storm surges associated with the passage of cold fronts, which are out of the scope of the present study. So, before computing the error metrics, a high-pass filter was applied to the observed water level series to remove the subtidal band comprised of harmonic components with periods >30 hours (Schettini et al. 2019; Ruiz et al. 2021). A scatter plot comparing modeled and observed water level at the calibration point (Praticagem Santos) for the period July–December 2012 is presented in Figure 4a. The model was then validated against water level observations at Ilha das Palmas for May–November 2012 (Figure 4b). The error metrics of the calibration and validation water level data are summarized in Table 5. Calibration was achieved up to a MAE of about 0.07 m and resulted in a similar value for the validation data. The PCC and slope that approach unity suggest low systematic bias. Results for both points show an overall good agreement with astronomical tides for the inner and outer regions of Santos Bay.

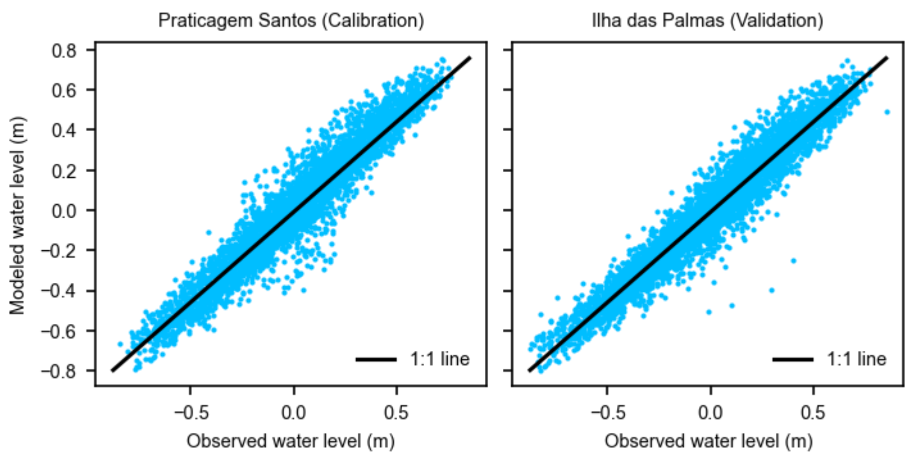

Figure 4: Scatter plots of modeled versus observed (tide gauge) water level for Praticagem Santos and Ilha das Palmas.

Table 5: Computed error metrics for water level and wave variables.

Metric	Water level (calibration) (m)	Water level (validation) (m)	Wave height (m)
ME	0.0069	−0.0033	0.0129
MAE	0.0689	0.0695	0.1352
PCC	0.9597	0.9639	0.8846
Slope	0.9797	0.9328	0.7845

The wave model was validated against the wave time series from the buoy in Santos Bay. A comparison between modeled and observed significant wave height for March–May 2016 is presented in Figure 5. Although wave height shows an overall good agreement (PCC of 0.88;

Table 5), on April 27 the buoy recorded an event with significant wave heights of up to 4 m that was not reproduced by the model (Figure 5a,b). This can be explained by extreme conditions underestimated (smoothed) by global wind and wave reanalyses (see, e.g., Stopa 2018) or by not simulating the wave-surge-tide interaction (Wolf 2009). Although the model did not reproduce the 4 m extreme waves, as seen in the next section, wave heights of 2 m are enough to resuspend virtually all the outfall sediment. Wave action stronger than that would further resuspend the underlying natural sediment, which was not considered in the present model. Furthermore, according to linear wave theory, the depth at which waves can effectively stir up the bed sediment depends to a greater extent on wavelength than on wave height.

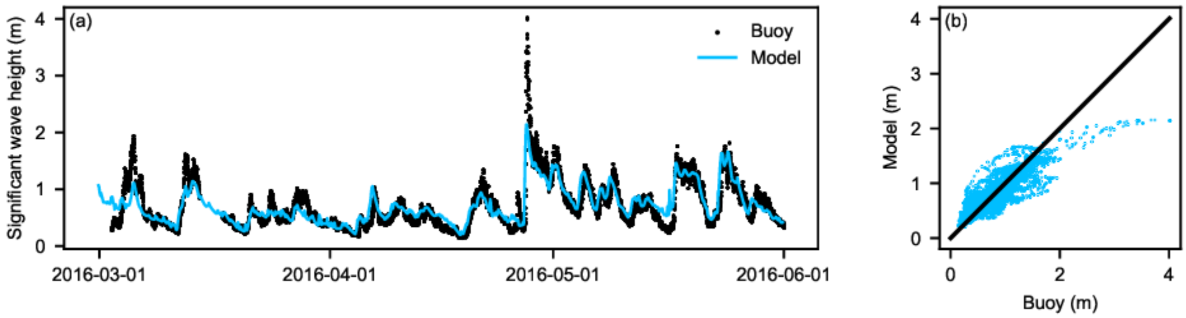

Figure 5: Time series (a) and scatter plot (b) of significant wave height in Santos Bay.

3.2. Sediment transport

The sum of the cohesive and non-cohesive fractions was computed from the model to give the total sediment concentration in the water column. Since this quantity is highly variable over time, being dominated by the outfall plumes, the temporal mean of each cell was calculated along the domain. Figure 6 shows a comparison of the time-averaged total sediment concentration between the current-only hydrodynamic model and the coupled wave-current model for the three sub-periods (January, March and July 2019). It can be observed that, among the five submerged outfalls, the outfall in Santos Bay has the largest sediment plume for all the sub-periods. This result is expected because the Santos outfall has the highest discharge and the highest concentration of total suspended solids. Interestingly, under the influence of waves, all outfalls exhibit more dispersed plumes, reaching higher concentrations in areas where sediment would be on average more diluted under the no-waves condition. This effect is more pronounced with mean and strong wave conditions (March and July). Since the effluent discharges and the suspended solids concentrations are kept constant between current-only and wave-current scenarios, this result must be associated with wave action.

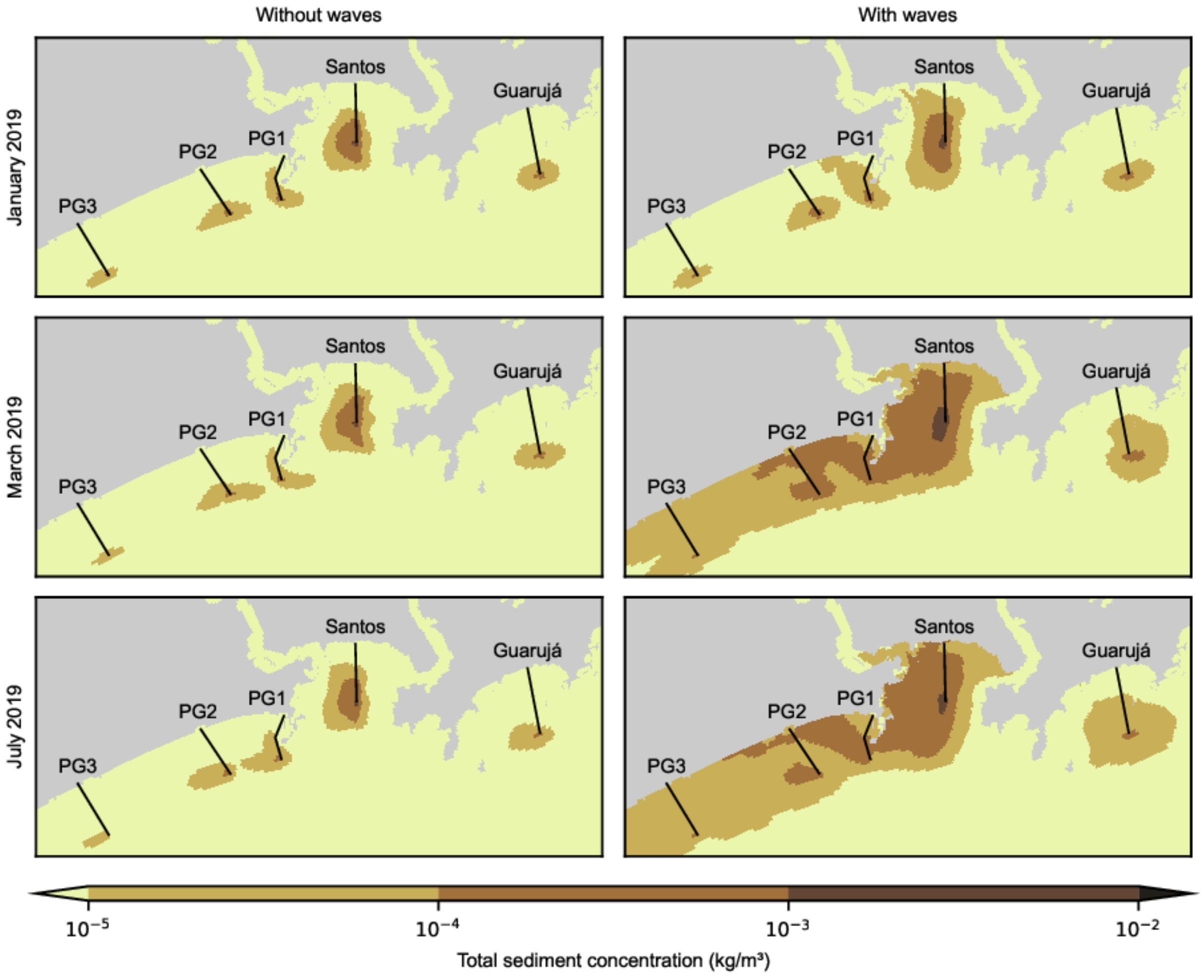

Figure 6: Temporal mean of total modeled sediment concentration with and without waves.

The extension of the sediment plumes under the influence of waves is not surprising. As illustrated by Magris et al. (2019), sediment discharges from land-based activities can produce plumes of fine-grained sediment that extend up to hundreds of kilometers from the release point, reaching nearby shores. This is reasonable given the conservative nature of sediment as a constituent. However, due to settling and dilution, the discharged sediment can rapidly reach concentrations below reference ambient levels, perhaps posing negligible impacts on the environment. In fact, suspended solids in the outfall effluents are $\mathcal{O}(10^{-1}\,\mathrm{kg/m^3})$ and, after release, get rapidly diluted up to $\mathcal{O}(10^{-3}\,\mathrm{kg/m^3})$ and lower, which is below ambient concentrations, i.e., $\mathcal{O}(10^{-2}\,\mathrm{kg/m^3})$ (Berzin 1992).

The contribution of cohesive and non-cohesive sediment fractions to the total modeled sediment concentration is shown in Figure 7 for mean wave conditions, i.e., March 2019. It can be observed that the cohesive fraction dominates the total sediment concentration (Figure 6). This occurs for two main reasons. First, cohesive sediment constitutes 81% of the total sediment concentration in the effluents. Second, due to their fine-grained nature, cohesive particles take more time to settle than non-cohesive sediment. The latter allows the particles to be transported further from the discharge location before intercepting the seabed.

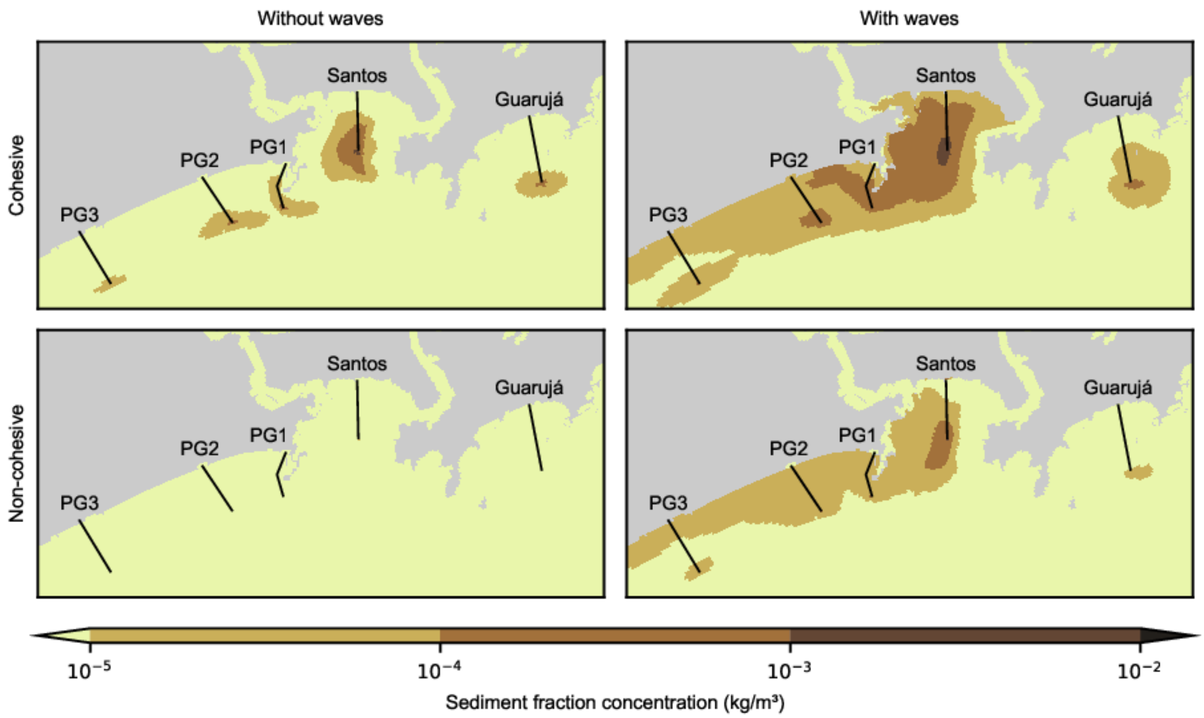

Figure 7: Temporal mean of modeled cohesive and non-cohesive sediment concentration for March 2019 with and without waves.

The modeled mass of cohesive and non-cohesive sediment deposited at the seabed is presented in Figure 8, also for March 2019 (mean wave conditions). Deposition for both fractions appears to be consistent with the corresponding plumes in Figure 7. For example, without the influence of waves, non-cohesive sediment rapidly settles in a small area around the diffuser for all five outfalls, producing negligible concentrations in the water column (of the order of 10^{-5} kg/m^3 and lower; see Figure 7). The cohesive fraction, however, gets more initial dispersion, and most of the deposition occurs within 1 km to 2 km from the diffusers. On the other hand, when considering the effect of waves, both fractions get highly dispersed over the domain. In particular, the non-cohesive fraction shows a drastic difference in plume extension, suggesting that wave action reentrains most of this sediment to the water column.

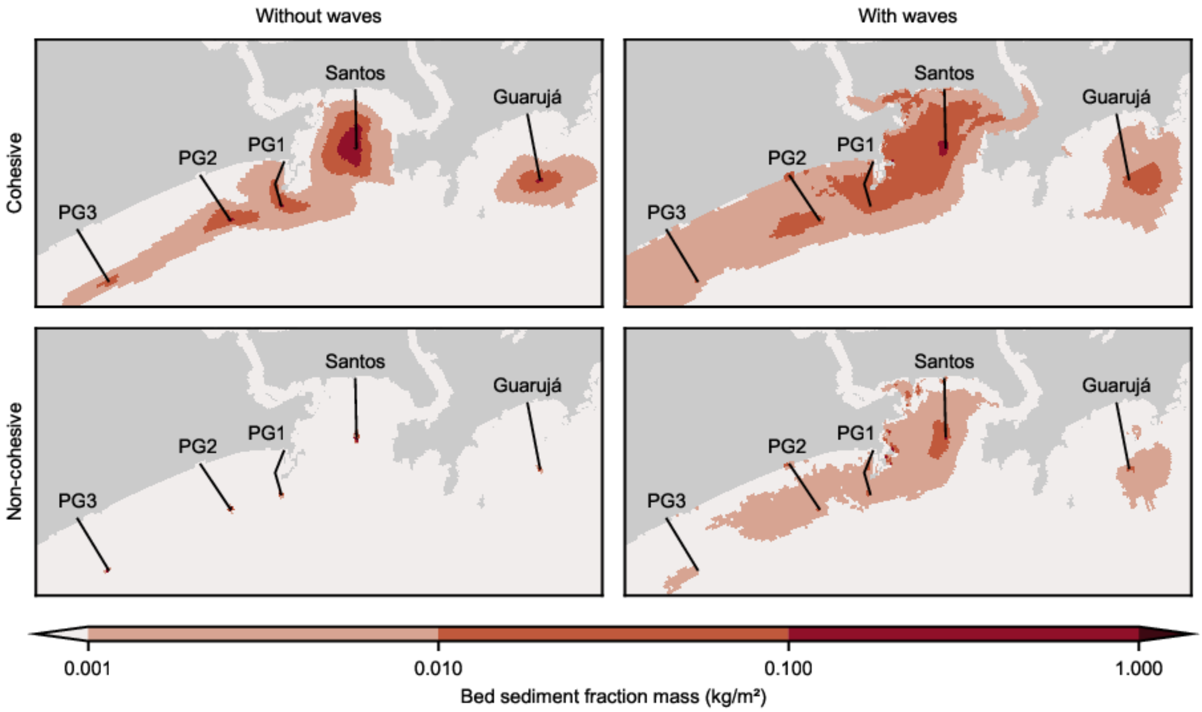

Figure 8: Modeled sediment deposition at the end of March 2019 with and without waves.

The deposited sediment mass (kg/m^2) was converted to sediment layer thickness (m) using the dry densities of cohesive and non-cohesive fractions. Deposition quantities expressed in terms of thickness are more intuitive and easier to reason about than mass per area, so, in Figure 9, the modeled bed sediment layer thickness at the end of the three sub-periods is presented. From observing Figure 9, it is evident that waves play a significant role in outfall sediment dispersion, affecting the final geometry of the deposits at the end of the sub-periods. Under wave influence, outfall sediment is mobilized over greater distances from the discharge point, reaching the entrance of the estuarine channels of São Vicente and Santos, and the coasts to the west. This is consistent with sediment plumes in Figure 6, especially under mean and strong wave regimes, where sediment is transported by westerly longshore currents. The overall deposition in the Santos Bay is compatible with a sedimentation sector that Fukumoto, Mahiques, and Tessler (2006) identified in the mid-western part of the bay and consists mainly of organic-rich facies. Indeed, Fukumoto, Mahiques, and Tessler (2006) proposed the influence of the Santos submerged outfall as one of the factors associated to this deposition area.

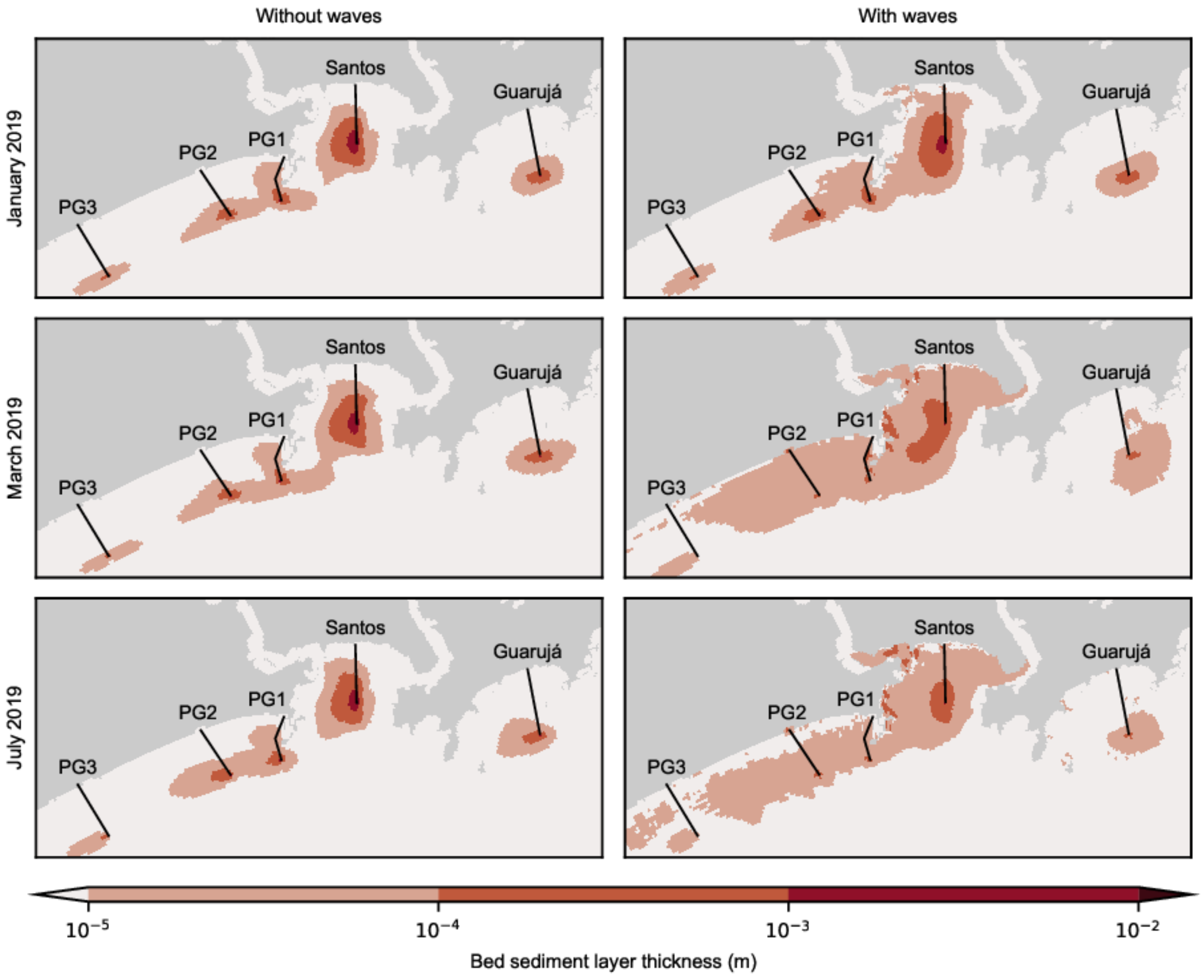

Figure 9: Modeled sediment deposition at the end of the sub-periods with and without waves.

The order of magnitude of the modeled sediment layer thickness is also shown in Figure 9. Without the influence of waves, the Santos outfall produces a thicker bed sediment layer, up to $\mathcal{O}(1\ \text{cm})$ in a small area in the vicinity of the diffuser, while the outfalls of Guarujá, PG1, PG2 and PG3 showed maximum depositions of $\mathcal{O}(1\ \text{mm})$. The location of the peak thickness is in the vicinity of the diffuser for all five outfalls, and this behavior remains unchanged between the current-only and wave-current models. In the months of March and July, the order of magnitude of the sediment layer thickness is greatly influenced by wave action; the sediment becomes distributed over larger areas with a lower thickness.

Events of sediment resuspension were found while analyzing the evolution of the modeled bed sediment layer near the outfall diffusers (Figure 10). Resuspension due to combined waves and currents occurs in the first and third weeks of January 2019, around days 5 and 20, for all outfalls. A less significant event of resuspension is observed on day 10. In July 2019, resuspension is more persistent, showing only a brief period of undisturbed deposition around the second week. The observed events of wave-generated resuspension can explain the increased sediment concentrations in the water column (Figure 6) because, once reentrainment occurs, sediment is further transported by currents.

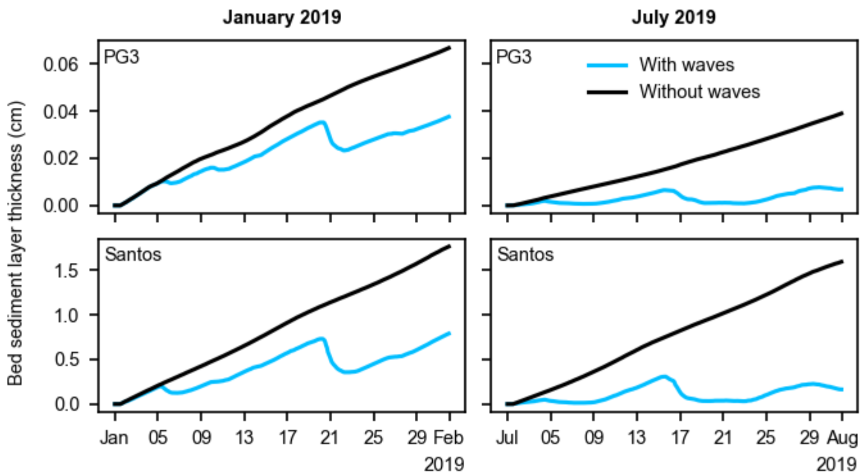

Figure 10: Evolution of the modeled bed sediment layer in the vicinity of the diffusers.

The outfalls of Santos and PG3 showed the highest and lowest final sediment deposition, respectively, coinciding with the magnitude of their discharges. Without wave effects, the Santos outfall produced a final deposition of 1.76 cm, and PG3 had only 0.07 cm at the end of January (mild wave conditions). However, considering waves, sediment deposition suffers reductions between 36% and 55%. With waves, the final deposition in January 2019 for Santos resulted in 0.79 cm, and in PG3 it was about 0.04 cm. On the other hand, considering the strong wave action of July, the sediment layer in Santos drops from 1.59 cm to 0.16 cm (−90%), and in PG3 it goes from 0.04 cm to 0.01 cm (−83%). This supports a relationship between the strength of wave conditions and the amount of resuspension. Also, those differences in sediment layer thickness indicate that, due to the action of waves, a large part of the sediment is removed from the location of initial deposition, preventing continued accumulation. In general, it can be noted that the deposition patterns are consistent among the five outfalls; they all show similar trends of sedimentation and erosion, only varying in magnitude. So, for the sake of brevity, from now on, only results for the Santos outfall will be presented.

As observed in Figure 10, the undisturbed depositional trend is approximately linear. However, a detailed view of the modeled deposition rate near the Santos outfall diffuser (Figure 11) shows that it has oscillation modes associated with the tidal motion. The average deposition rate is between 0.05 cm/day and 0.06 cm/day for the three sub-periods. At such an accelerated rate, after a whole year, an undisturbed deposition would result in a modeled sediment layer of about 20 cm. Due to wave action, deposition in the model is frequently hindered and interrupted, preventing the formation of unrealistic sediment deposits in the long term.

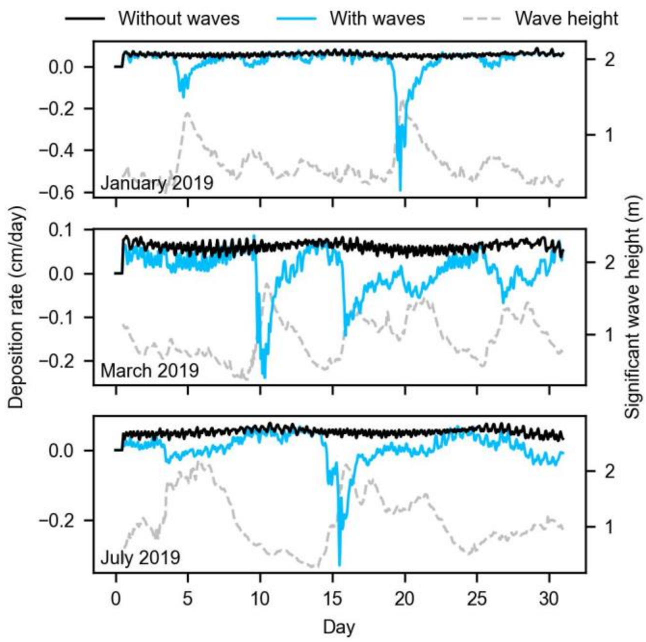

Figure 11: Modeled deposition rate in the vicinity of the Santos outfall diffuser.

In periods of reduced wave action, the deposition rate under calm conditions is approximately the same between the standalone hydrodynamic model and the coupled wave-current model (see, e.g., January 2019 in Figure 11). Figure 11 also shows that after events of resuspension (rate below zero) the deposition process tends to regain the initial rate. This behavior suggests that, in the model, waves do not have a significant effect on the deposition rate per se and only cause temporary disruptions. Nevertheless, in March and July, wave conditions are strong enough to hinder deposition during most of the sub-period.

In the present model, outfall sediment transport takes place over a fixed bed, and sediment resuspension is limited by the available outfall sediment at bed. For example, in January 2019, there is more time of undisturbed deposition, so the available resuspendable sediment is greater. That is why January 2019 shows a more intense resuspension event than March and July 2019 (−0.6 cm/day; see Figure 11). Sediment resuspension also depends on the grain size distribution because sand-sized sediment is easier to resuspend due to its non-cohesive nature. For instance, since non-cohesive sediment tends to settle closer to the diffusers than cohesive sediment (as illustrated in Figure 8), resuspension rates in the vicinity of the outfalls are controlled by non-cohesive sediment.

Since sediment resuspension is dominated by the bed shear stress, it is expected that the interaction of waves and currents induces higher stresses. Indeed, around July 7, the bed shear stress in the wave-current model was an order of magnitude higher than in the standalone hydrodynamic model (see Figure A4 in Appendix). The enhancement of bed shear stresses is produced by a non-linear combination of current and wave stresses, which results in time-averaged and maximum components of oscillatory stress (Soulsby et al., 1993). Wave propagation can force currents, increasing their velocity and associated time-averaged stress; however, waves themselves produce a progressive orbital motion that controls the maximum component of oscillatory stress. The contribution of those two mechanisms can be assessed by comparing the overall increase in current velocity due to the inclusion of waves and the near-bottom wave orbital velocity. Current velocities in Figure 12b are slightly affected by wave action because outfall diffusers are located offshore outside of the surf zone, in areas where radiation stresses are not able to drive significant currents. On the other hand, near-bed orbital velocities at the same location (Figure 12c) have pronounced peaks with higher magnitudes than those of currents. Strong near-bottom orbital motion can stir up bed sediments, producing the resuspension events observed in Figure 12a. This indicates that the dominant process for the enhancement of bed shear stress is the orbital motion of waves.

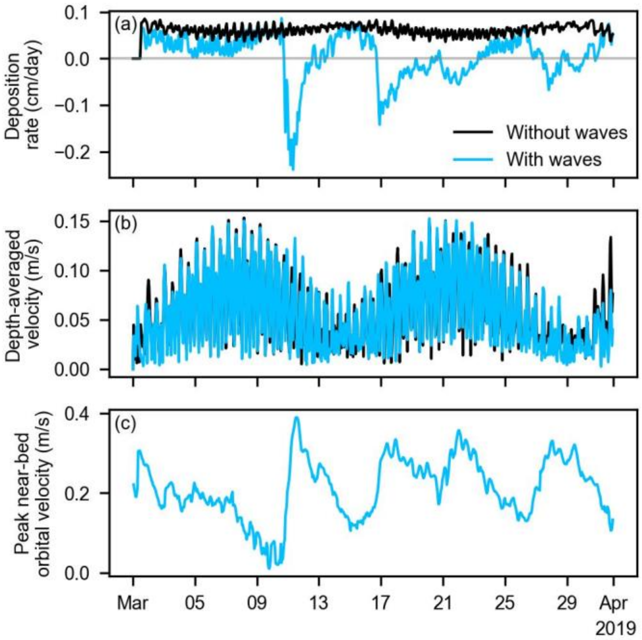

Figure 12: Modeled deposition rate (a), depth-averaged velocity (b) and peak near-bottom orbital velocity (c) in the vicinity of the Santos outfall diffuser in March 2019.

According to linear wave theory, the lower limit of wave action is at a depth equal to half the wavelength. Waves propagating over water deeper than this limit are deep-water waves. The effect of deep-water waves on the seabed is negligible; however, once the waves reach shallower depths, they begin to interact with the seabed. Figure 13 presents the depth-wavelength ratio of waves near the Santos outfall diffuser and the lower limit that corresponds to a ratio of 0.5. In January 2019, waves are in the deep-water regime most of the time with brief incursions into a transitional regime (<0.5) in which near-bed elliptical motions can stir up bed sediment. On the other hand, in March and July, waves are mostly in the intermediate regime. Since March is representative of mean wave conditions, resuspension events and hindered deposition can be expected throughout most of the year. Furthermore, by comparing the occurrence of resuspension events (negative deposition ratios) with wave conditions, it is found that resuspension can occur under significant wave heights as low as 0.57 m with mean wave periods of 5.5 s in January.

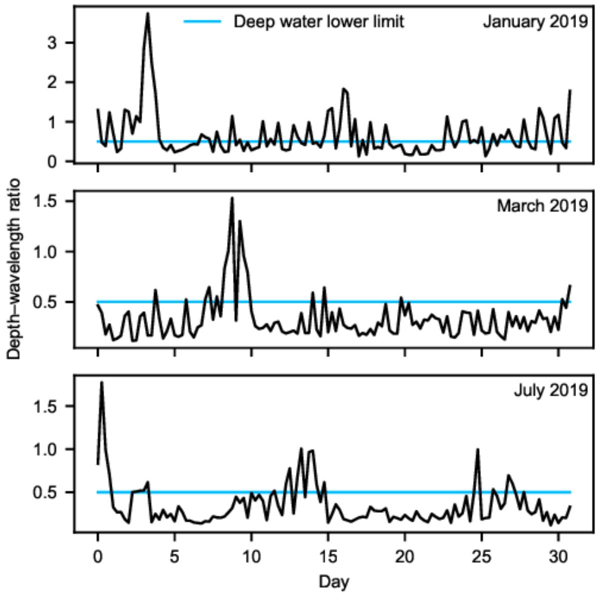

Figure 13: Modeled depth-wavelength ratio in the vicinity of the Santos outfall diffuser.

4. Conclusions and recommendations

A coupled wave-current model with sediment transport was implemented in order to study the effects of waves on the transport and fate of sediments from submerged outfalls in relatively shallow waters. As a case study, an ensemble of five submerged outfalls in the coastal area of Baixada Santista, São Paulo state, Brazil, was selected. The model was implemented using operational data for 2019 provided by Sabesp. Comparison of results from a standalone hydrodynamic model (without waves) and the coupled wave-current model of Baixada Santista shows that waves have significant effects on the transport and fate of outfall solid particles

If waves are not considered, the model simulates a continuous deposition process that, in the long term, results in unrealistic sediment deposits (about 20 cm/year for the Santos outfall). It was found that events of wave-induced sediment resuspension can occur in the vicinity of the outfall diffusers, even during the austral summer (January 2019), when waves are less energetic. In other seasons, waves are generally strong enough to hinder deposition and to remobilize sediment most of the time; for example, in months of average wave action and during the winter (March and July 2019, respectively). When considering wave-current interaction, after a month of simulation, bed sediment deposits were up to 55% thinner under mild wave conditions and up to 90% thinner under strong waves.

The action of waves causes sediment to be dispersed over larger extents. If waves are not included in the model, outfall sediments tend to settle within 1 km to 2 km from the diffusers. However, with wave-induced resuspension, the reentrained sediment is transported further, reaching beaches and channels and eventually settling there. Furthermore, under mean and strong wave conditions, it was found that resuspended sediment can be transported westward over greater distances by wave-induced longshore currents. This affects the overall temporal distribution of sediment concentration in the water column in a way that relatively higher concentrations are more persistent over time.

The observed events of sediment resuspension respond to an increase in bed shear stresses due to wave-current interaction. At the depth of the diffusers, wave radiation stresses are not able to significantly intensify currents, but on average waves are large enough to produce elevated near-bed orbital velocities. The elliptical orbital motion of waves in the area can stir up bed sediments and reentrain them in the water column as a result from a non-linear interaction between current and wave bed boundary layers. These findings were found to be consistent with linear wave theory.

The present study was not aimed to accurately quantify outfall sediment deposition nor to assess the environmental impacts of these sediments. However, results provide phenomenological insights that may serve as a baseline for future studies on the matter. In order to evaluate potential impacts, it is necessary to perform detailed simulations of the sediment transport in the beaches and channels and accurately estimate sediment deposition. Since sediment transport is a complex process, especially for fine and silt-sized sediments such as those found in the effluents, a more detailed model implementation could be beneficial. However, this would require additional laboratory analyses to determine settling velocity, salinity-induced sediment flocculation and empirical parameters for sedimentation and erosion, as implemented in Delft3D (Deltares 2020a). Additionally, a coupled water-sediment quality model could be implemented to study the interaction of wastewater pollutants with sediment particles. For example, taking into account sediment-attached fecal bacteria as a source or sink of bacteria concentration for the water column (e.g., Gao, Falconer, and Lin 2013). This must be paired with sediment tracer studies (e.g., Pearson et al. 2021) to calibrate and validate the outfall sediment transport model. This would allow to assess actual environmental concerns.

The effects of strong extreme waves generated by meteorological events such as cold fronts and storms must be investigated because they have a high potential for outfall sediment resuspension. Storm systems can produce waves with very long periods that can easily resuspend sediments at water depths that are normally under a deep-water wave regime. In fact, storm-induced waves can stir up fine sediments at depths of up to 40 m (Roberts et al. 2010). Furthermore, efforts could be done in integrating models of near-field sediment deposition from marine outfall jets (e.g., M. J. Neves and Fernando 1995; Bleninger and Carmer 2000; Lane-Serff and Moran 2005; Cuthbertson et al. 2008; Terfous, Chiban, and Ghenaim 2016) to coupled near-far-field modelling systems (e.g., Bleninger 2006; Morelissen, van der Kaaij, and Bleninger 2013; Horita et al. 2019). This would allow for a very detailed simulation of the non-linear interaction between currents, waves, sediment and outfall jets/plumes.

It is suggested that future studies consider the potential effects of surface waves on the design and operational conditions of submerged sewage outfalls. In particular, for outfalls that discharge in relatively shallow waters, the local wave climate must be analyzed to assess the potential for sediment resuspension. The results of coupled wave-current far-field models of outfall effluents can allow for understanding the fate of sediment-attached contaminants and identifying areas of potential environmental concern under differing current and future scenarios.

Acknowledgements

The authors are grateful to the Sanitation Company of São Paulo State (Sabesp) ~~and~~, Fundação Centro Tecnológico de Hidráulica (FCTH), and the former Companhia Docas do Estado de São

Paulo (Codesp) for providing valuable data. D.A.C. thanks the Brazilian Coordination for the Improvement of Higher Education Personnel (CAPES Foundation) for providing him with a scholarship for full-time commitment to the research. T.B. acknowledges the productivity stipend from the Brazilian Council for Scientific and Technological Development (CNPq), grant 312211/2020-1, call 09/2020.

Disclosure statement

The authors report there are no competing interests to declare.

Data availability statement

Data will be made available on request.

Biographical note

Diego Casas is a doctoral student in the Graduate Program of Water Resources and Environmental Engineering (PPGERHA) at the Federal University of Paraná (UFPR) in Curitiba, Brazil, where he also completed his master's studies (2023). He is a civil engineer who graduated from Universidad del Norte, Colombia (2020), and worked on consultancy projects in water resources engineering. His research is on the effects of waves on environmental processes such as the transport and fate of constituents and the exchange of momentum at the air-water interface.

Tobias Bleninger is professor (2011) for Environmental Fluid Mechanics, and Applied Mathematics at the Department of Environmental Engineering of the Federal University of Paraná (UFPR) in Curitiba, Brazil. He is a Civil Engineer (2000) from the Karlsruhe Institute of Technology (KIT), Germany, where he did his Doctor in Environmental Fluid Mechanics (2006) and lead the research group of Environmental Fluid Mechanics of the Institute for Hydromechanics (2007–2011). Tobias Bleninger has experience in Hydraulics and Fluid Mechanics, with focus on physical and numerical modelling of Mixing and Transport Processes of Environmental Fluid Systems.

Maurício F. Gobbi holds a bachelor's degree in civil engineering from the Federal University of Rio de Janeiro (1990), a master's degree in Ocean Engineering from the Federal University of Rio de Janeiro (1993) and a doctorate in Coastal and Oceanographic Engineering from the University of Delaware (1997). He is currently professor at the Federal University of Paraná in the undergraduate program in Environmental Engineering, the Graduate Program in Numerical Methods in Engineering and the Graduate Program in Environmental Engineering. He has experience in Environmental Engineering, with an emphasis on Environmental Fluid Mechanics, Coastal and Oceanographic Engineering, Water Quality, Environmental Hydrology, Numerical Modeling in Fluid Mechanics, working mainly on the following topics: wave propagation in coastal environments, hydrodynamics and water quality of water bodies, atmospheric modeling, hydrological modeling, high performance computing.

Silene Baptistelli has a degree in Civil Engineering from the Armando Álvares Penteado Foundation (1990), a master's degree in civil engineering from the University of São Paulo (2003) and a doctorate in civil engineering from the University of São Paulo (2008). She is currently a Civil Engineer at the Sanitation Company of São Paulo State (Sabesp) and a lecturer at Mackenzie Presbyterian University on Graduate Course in Construction Project Management. She has experience in Civil Engineering, with an emphasis on Sanitary, Hydraulic and Environmental Engineering, working mainly on the following subjects: basic sanitation, water supply systems, sewage systems, marine hydraulics, effluent dispersion, environmental management, water resources management and numerical modeling.

References

Abessa, D. M. S., R. S. Carr, B. R. F. Rachid, E. C. P. M. Sousa, M. A. Hortelani, and J. E. Sarkis. 2005. "Influence of a Brazilian Sewage Outfall on the Toxicity and Contamination of Adjacent Sediments." *Marine Pollution Bulletin* 50 (8): 875–85. https://doi.org/10.1016/j.marpolbul.2005.02.034.

Abessa, D. M. S., R. S. Carr, E. C. P. M. Sousa, B. R. F. Rachid, L. P. Zaroni, M. R. Gasparro, Y. A. Pinto, et al. 2008. "Integrative Ecotoxicological Assessment of Contaminated Sediments in a Complex Tropical Estuarine System." In *Marine Pollution: New Research*, edited by Tobias N. Hofer, 279–312. New York: Nova Science Publishers, Inc.

Akdemir, Tolga, and Goktug Dalgic. 2021. "The Impact of the Marine Sewage Outfalls on the Sediment Quality: The Black Sea and the Marmara Case." *Saudi Journal of Biological Sciences* 28 (1): 238–46. https://doi.org/10.1016/j.sjbs.2020.09.055.

Allard, Richard, W. Erick Rogers, Suzanne N. Carroll, and Kate V. Rushing. 2004. "Validation Test Report for the Simulating Waves Nearshore Model (SWAN): Cycle III, Version 40.11." Formal report NRL/FR/7320--04-10,070. Stennis Space Center, MS: Naval Research Laboratory.

Alosairi, Y., T. Pokavanich, and N. Alsulaiman. 2018. "Three-Dimensional Hydrodynamic Modelling Study of Reverse Estuarine Circulation: Kuwait Bay." *Marine Pollution Bulletin* 127:82–96. https://doi.org/10.1016/j.marpolbul.2017.11.049.

Arifin, A. N., S. Yano, and A. T. Lando. 2020. "Assessing Effects of Temporal Changes in River Water Temperature on Stratification in the Ariake Sea." *IOP Conference Series: Earth and Environmental Science* 419 (1): 012157. https://doi.org/10.1088/1755-1315/419/1/012157.

Ashley, Richard M., and T. Hvitved-Jacobsen. 2003. "Management of Sewer Sediments." In *Wet-Weather Flow in the Urban Watershed: Technology and Management*, edited by Richard Field and Daniel Sullivan. Boca Raton, FL: Lewis Publishers.

Avnimelech, Yoram, Gad Ritvo, Leon E. Meijer, and Malka Kochba. 2001. "Water Content, Organic Carbon and Dry Bulk Density in Flooded Sediments." *Aquacultural Engineering* 25 (1): 25–33. https://doi.org/10.1016/s0144-8609(01)00068-1.

Aydoğan, Burak, and Berna Ayat. 2021. "Performance Evaluation of SWAN ST6 Physics Forced by ERA5 Wind Fields for Wave Prediction in an Enclosed Basin." *Ocean Engineering* 240:109936. https://doi.org/10.1016/j.oceaneng.2021.109936.

Baptistelli, Silene Cristina. 2015. "Hydrodynamic Modeling: Mpplication of Delft3D-FLOW in Santos Bay, São Paulo State, Brazil." In *Recent Progress in Desalination, Environmental and Marine Outfall Systems*, 307–32. Cham, Switzerland: Springer International Publishing. https://doi.org/10.1007/978-3-319-19123-2_22.

Belém, André Luiz, Gleyci Aparecida Oliveira Moser, Maria Fernanda Palanch-Hans, Frederico Fabio Mauad, and Liliane Lazzari Albertin. 2007. "Circulação/Estratificação Transiente No Complexo Estuarino de Santos: Comparações Entre o Estuário Interno e Área Costeira Adjacente Durante Sizigia." In *Anais Do XVII Simpósio Brasileiro de Recursos Hídricos*, 1–7. São Paulo, Brazil: Associação Brasileira de Recursos Hídricos (ABRHidro).

Berbel, Gláucia Bueno Benedetti, Marcos Antonio Hortellani, Jorge Eduardo de Souza Sarkis, Vitor Gonsalez Chiozzini, Deborah Inês Teixeira Fávaro, Bruno Otero Sutti, Nixon Claudio Sakazaki, and Elisabete de Santis Braga. 2021. "Emerging Contaminants (Rh, Pd, and Pt) in Surface Sediments from a Brazilian Subtropical Estuary Influenced by Anthropogenic Activities." *Marine Pollution Bulletin* 163:111929. https://doi.org/10.1016/j.marpolbul.2020.111929.

Berzin, G. 1992. "Monitoring of the Santos Submarine Outfall, São Paulo, Brazil, 10 Years in Operation." *Water Science and Technology* 25 (9): 59–71. https://doi.org/10.2166/wst.1992.0206.

Birocchi, Paula, Marcelo Dottori, Carine de Godoi Rezende Costa, and José Roberto Bairão Leite. 2021. "Study of Three Domestic Sewage Submarine Outfall Plumes through the Use of Numerical Modeling in the São Sebastião Channel, São Paulo State, Brazil." *Regional Studies in Marine Science* 42:101647. https://doi.org/10.1016/j.rsma.2021.101647.

Bleck, Rainer. 2002. "An Oceanic General Circulation Model Framed in Hybrid Isopycnic-Cartesian Coordinates." *Ocean Modelling* 4 (1): 55–88. https://doi.org/10.1016/S1463-5003(01)00012-9.

Bleninger, Tobias. 2006. "Coupled 3D Hydrodynamic Models for Submarine Outfalls: Environmental Hydraulic Design and Control of Multiport Diffusers." Ph.D. thesis, Karlsruhe, Germany: University of Karlsruhe. https://doi.org/10.5445/KSP/1000006668.

Bleninger, Tobias, and Carl Fr. v. Carmer. 2000. "Sedimentation in Particle-Laden-Jets." Diploma thesis, Karlsruhe, Germany: University of Karlsruhe.

Bodeen, C. A., T. J. Hendricks, W. E. Frick, D. J. Baumgartner, J. E. Yerxa, and A. Steele. 1989. *User's Guide for SEDDEP: A Program for Computing Seabed Deposition Rates of Outfall Particulates in Coastal Marine Environments*. Marine Science Center, U.S. Environmental Protection Agency. https://nepis.epa.gov/Exe/ZyPURL.cgi?Dockey=910096B9.txt.

Booij, N., R. C. Ris, and L. H. Holthuijsen. 1999. "A Third-Generation Wave Model for Coastal Regions: 1. Model Description and Validation." *Journal of Geophysical Research: Oceans* 104 (C4): 7649–66. https://doi.org/10.1029/98JC02622.

Bose, Nícolas de A., Marília S. Ramos, Gustavo S. Correia, Claus W. Saidelles, Leandro Farina, Claudia K. Parise, and João L. Nicolodi. 2022. "Assessing Wind Datasets and Boundary

Conditions for Wave Hindcasting in the Southern Brazil Nearshore." *Computers & Geosciences* 159:104972. https://doi.org/10.1016/j.cageo.2021.104972.

Bouws, E., and G. J. Komen. 1983. "On the Balance between Growth and Dissipation in an Extreme Depth-Limited Wind-Sea in the Southern North Sea." *Journal of Physical Oceanography* 13 (9): 1653–58. https://doi.org/10.1175/1520-0485(1983)013<1653:otbbga>2.0.co;2.

Boyd, Claude E. 1995. *Bottom Soils, Sediment, and Pond Aquaculture*. New York: Chapman & Hall.

Cesar, Augusto, Camilo Dias Seabra Pereira, Aldo Ramos Santos, Denis Moledo de Sousa Abessa, Nuria Fernández, Rodrigo Brasil Choueri, and Tomaz Angel DelValls. 2006. "Ecotoxicological Assessment of Sediments from the Santos and São Vicente Estuarine System – Brazil." *Brazilian Journal of Oceanography* 54 (1).

CETESB. 2022. "Qualidade Das Águas Costeiras No Estado de São Paulo 2021." Report. São Paulo, Brazil: Companhia de Tecnologia de Saneamento Ambiental (CETESB).

Consórcio Partner/TetraTech. 2017. "Estudo de Concepção de Alternativas Tecnológicas de Tratamento de Esgotos e de Resíduos Sólidos Nos Sistemas de Esgotos Da Área Insular Dos Municípios de Santos e São Vicente. Volume II de II: Modelagem de Transporte de Sedimento." Final report.

Correndo, Adrian A., Trevor J. Hefley, Dean P. Holzworth, and Ignacio A. Ciampitti. 2021. "Revisiting Linear Regression to Test Agreement in Continuous Predicted-Observed Datasets." *Agricultural Systems* 192:103194. https://doi.org/10.1016/j.agsy.2021.103194.

Cuthbertson, Alan J. S., David D. Apsley, Peter A. Davies, Giordano Lipari, and Peter K. Stansby. 2008. "Deposition from Particle-Laden, Plane, Turbulent, Buoyant Jets." *Journal of Hydraulic Engineering* 134 (8): 1110–22. https://doi.org/10.1061/(ASCE)0733-9429(2008)134:8(1110).

Deltares. 2020a. *Delft3D-FLOW, User Manual, Version 3.15*. Delft, Netherlands: Deltares.

———. 2020b. *Delft3D-WAVE, User Manual, Version 3.05*. Delft, Netherlands: Deltares.

Egbert, Gary D., and Svetlana Y. Erofeeva. 2002. "Efficient Inverse Modeling of Barotropic Ocean Tides." *Journal of Atmospheric and Oceanic Technology* 19 (2): 183–204. https://doi.org/10.1175/1520-0426(2002)019<0183:EIMOBO>2.0.CO;2.

Elias, E. P. L., D. J. R. Walstra, J. A. Roelvink, M. J. F. Stive, and M. D. Klein. 2001. "Hydrodynamic Validation of Delft3D with Field Measurements at Egmond." In *Coastal Engineering 2000: Conference Proceedings*, edited by Billy L. Edge, 2714–27. Sydney, Australia: American Society of Civil Engineers. https://doi.org/10.1061/40549(276)212.

Escobar, Gustavo Carlos Juan, Michelle Simões Reboita, and Amanda Souza. 2019. "Climatology of Surface Baroclinic Zones in the Coast of Brazil." *Atmósfera* 32 (2): 129–41. https://doi.org/10.20937/ATM.2019.32.02.04.

Falkenberg, A. V., R. C. Barletta, L. Franklin, P. Ribeiro, P. G. De Lara, T. Bleninger, A. B. Trevisan, and V. Dos Santos. 2016. "Optimizing Outfall System Configurations Using Decision Support and Numerical Models. Case Study of Santa Catarina Island, Brazil." In *Proceedings of the International Symposium on Outfall Systems, 2016*, 1–10. Ottawa, Canada: IAHR. https://www.iahr.org/library/infor?pid=9171.

Ferré, Bénédicte, Christopher R. Sherwood, and Patricia L. Wiberg. 2010. "Sediment Transport on the Palos Verdes Shelf, California." *Continental Shelf Research* 30 (7): 761–80. https://doi.org/10.1016/j.csr.2010.01.011.

Fukumoto, M. M., M. M. Mahiques, and M. G. Tessler. 2006. "Bottom Faciology and Sediment Transport in Santos Bay, Southeastern Brazil." In *Journal of Coastal Research, Special Issue No. 39. Proceedings of the 8th International Coastal Symposium (ICS 2004)*, 3:1737–40.

Gao, Guanghai, Roger A. Falconer, and Binliang Lin. 2013. "Modelling Importance of Sediment Effects on Fate and Transport of Enterococci in the Severn Estuary, UK." *Marine Pollution Bulletin* 67 (1): 45–54. https://doi.org/10.1016/j.marpolbul.2012.12.002.

Gelaro, Ronald, Will McCarty, Max J. Suárez, Ricardo Todling, Andrea Molod, Lawrence Takacs, Cynthia A. Randles, et al. 2017. "The Modern-Era Retrospective Analysis for Research and Applications, Version 2 (MERRA-2)." *Journal of Climate* 30 (14): 5419–54. https://doi.org/10.1175/JCLI-D-16-0758.1.

Gerritsen, H., E. D. de Goede, F. W. Platzek, J. A. Th M. van Kester, M. Genseberger, and R. E. Uittenbogaard. 2008. "Validation Document Delft3D-FLOW, a Software System for 3D Flow Simulations." Final report. Delft, Netherlands: Deltares.

Gkaragkouni, Anastasia, Spyros Sergiou, Maria Geraga, Helen Papaefthymiou, Dimitrios Christodoulou, and George Papatheodorou. 2021. "Heavy Metal Distribution, Sources and Contamination Assessment in Polluted Marine Sediments: Keratsini Outfall Sewer Area, Saronikos Gulf, Greece." *Water, Air, & Soil Pollution* 232 (11): 477. https://doi.org/10.1007/s11270-021-05400-z.

Harari, J., C. França, and R. Camargo. 2008. "Climatology and Hydrography of Santos Estuary." In *Perspectives on Integrated Coastal Zone Management in South America*, 147–60. IST Press.

Hasselmann, K., T. P. Barnett, E. Bouws, H. Carlson, D. E. Cartwright, K. Enke, J. A. Ewing, et al. 1973. *Measurements of Wind-Wave Growth and Swell Decay during the Joint North Sea Wave Project (JONSWAP)*. Ergänzungsheft Zur Deutschen Hydrographische Zeitschrift, Reihe A 12. Hamburg, Germany: Deutsche Hydrographisches Institut.

Herring, James R. 1980. "Wastewater Particle Dispersion in the Southern California Offshore Region." In *Particulates in Water: Characterization, Fate, Effects, and Removal*, edited by Michael C. Kavanaugh and James O. Leckie, 283–304. Advances in Chemistry 189. Washington, D.C.: American Chemical Society.

Hersbach, Hans, Bill Bell, Paul Berrisford, Shoji Hirahara, András Horányi, Joaquín Muñoz-Sabater, Julien Nicolas, et al. 2020. "The ERA5 Global Reanalysis." *Quarterly Journal of the Royal Meteorological Society* 146 (730): 1999–2049. https://doi.org/10.1002/qj.3803.

Hershelman, G. P., H. A. Schafer, T.-K. Jan, and D. R. Young. 1981. "Metals in Marine Sediments near a Large California Municipal Outfall." *Marine Pollution Bulletin* 12 (4): 131–34. https://doi.org/10.1016/0025-326X(81)90442-2.

Hodgins, Donald O., Sandra L. M. Hodgins, and Richard E. Corbett. 2000. "Modeling Sewage Solids Deposition Patterns for the Five Fingers Island Outfall, Nanaimo, British Columbia." In *Proceedings of the Watershed Management 2000 Conference*, 991–1008. Water Environment Federation. https://doi.org/10.2175/193864700785149008.

Horita, Cristina Ono, Tobias Bernward Bleninger, Robin Morelissen, and João Luiz Baptista de Carvalho. 2019. "Dynamic Coupling of a near with a Far Field Model for Outfall Discharges." *Journal of Applied Water Engineering and Research* 7 (4): 295–313. https://doi.org/10.1080/23249676.2019.1685413.

Huff, Thomas P., Rusty A. Feagin, and Jens Figlus. 2022. "Delft3D as a Tool for Living Shoreline Design Selection by Coastal Managers." *Frontiers in Built Environment* 8. https://doi.org/10.3389/fbuil.2022.926662.

Inan, Asu. 2019. "Modeling of Hydrodynamics and Dilution in Coastal Waters." *Water* 11 (1). https://doi.org/10.3390/w11010083.

Innocentini, Valdir, Ernesto Caetano, and Jonas Takeo Carvalho. 2014. "A Procedure for Operational Use of Wave Hindcasts to Identify Landfall of Heavy Swell." *Weather and Forecasting* 29 (2): 349–65. https://doi.org/10.1175/waf-d-13-00077.1.

Iouzzi, Nisrine, Laila Mouakkir, Mouldi Ben Meftah, Mohamed Chagdali, and Dalila Loudyi. 2022. "SWAN Modeling of Dredging Effect on the Oued Sebou Estuary." *Water* 14 (17). https://doi.org/10.3390/w14172633.

Kaiser, Júlia, Izabel C. M. Nogueira, Ricardo M. Campos, Carlos E. Parente, Renato P. Martins, and Wellington C. Belo. 2022. "Evaluation of Wave Model Performance in the South Atlantic Ocean: A Study about Physical Parameterization and Wind Forcing Calibration." *Ocean Dynamics* 72 (2): 137–50. https://doi.org/10.1007/s10236-021-01495-4.

Kalnejais, Linda H., William R. Martin, and Michael H. Bothner. 2010. "The Release of Dissolved Nutrients and Metals from Coastal Sediments Due to Resuspension." *Marine Chemistry* 121 (1): 224–35. https://doi.org/10.1016/j.marchem.2010.05.002.

Kanamitsu, Masao, Wesley Ebisuzaki, Jack Woollen, Shi-Keng Yang, J. J. Hnilo, M. Fiorino, and G. L. Potter. 2002. "NCEP–DOE AMIP-II Reanalysis (R-2)." *Bulletin of the American Meteorological Society* 83 (11): 1631–44. https://doi.org/10.1175/BAMS-83-11-1631.

Kim, Minjeong, Mayzonee Ligaray, Yong Sung Kwon, Soobin Kim, Sangsoo Baek, JongCheol Pyo, Gahyun Baek, et al. 2021. "Designing a Marine Outfall to Reduce Microbial Risk on a Recreational Beach: Field Experiment and Modeling." *Journal of Hazardous Materials* 409:124587. https://doi.org/10.1016/j.jhazmat.2020.124587.

Lane-Serff, Gregory F., and Terry J. Moran. 2005. "Sedimentation from Buoyant Jets." *Journal of Hydraulic Engineering* 131 (3): 166–74. https://doi.org/10.1061/(ASCE)0733-9429(2005)131:3(166).

Lee, H. J., M. A. Noble, and J. Xu. 2003. "Sediment Transport and Deposition Processes near Ocean Outfalls in Southern California." In *Contaminated Sediments: Characterization, Evaluation, Mitigation/Restoration, and Management Strategy Performance*, edited by Jacques Locat, Rosa Galvez Cloutier, Ronald Chaney, and Kenneth Demars, 253–65. West Conshohocken, PA: ASTM International. https://doi.org/10.1520/STP11567S.

Lenstra, Klaas J. H., Stefan R. P. M. Pluis, Wim Ridderinkhof, Gerben Ruessink, and Maarten van der Vegt. 2019. "Cyclic Channel-Shoal Dynamics at the Ameland Inlet: The Impact on Waves, Tides, and Sediment Transport." *Ocean Dynamics* 69 (4): 409–25. https://doi.org/10.1007/s10236-019-01249-3.

Magris, Rafael, Martinho Marta-Almeida, José Monteiro, and Natalie Ban. 2019. "A Modelling Approach to Assess the Impact of Land Mining on Marine Biodiversity: Assessment in Coastal Catchments Experiencing Catastrophic Events (SW Brazil)." *Science of The Total Environment* 659:828–40. https://doi.org/10.1016/j.scitotenv.2018.12.238.

Maruya, Keith A., Doris E. Vidal-Dorsch, Steven M. Bay, Jeong W. Kwon, Kang Xia, and Kevin L. Armbrust. 2012. "Organic Contaminants of Emerging Concern in Sediments and Flatfish Collected near Outfalls Discharging Treated Wastewater Effluent to the Southern California Bight." *Environmental Toxicology and Chemistry* 31 (12): 2683–88. https://doi.org/10.1002/etc.2003.

Megahan, Walter F. 1999. "Sediment Pollution." In *Encyclopedia of Environmental Science*, edited by David E. Alexander and Rhodes W. Fairbridge. Encyclopedia of Earth Sciences. Dordrecht, Netherlands: Springer. https://doi.org/10.1007/1-4020-4494-1_297.

Mendes, Joana, Rui Ruela, Ana Picado, João Pedro Pinheiro, Américo Soares Ribeiro, Humberto Pereira, and João Miguel Dias. 2021. "Modeling Dynamic Processes of Mondego Estuary and Óbidos Lagoon Using Delft3D." *Journal of Marine Science and Engineering* 9 (1). https://doi.org/10.3390/jmse9010091.

Metcalf & Eddy. 2014. *Wastewater Engineering: Treatment and Resource Recovery*. Fifth edition. New York: McGraw-Hill Education.

Moon, Hyo-Bang, Sang-Pil Yoon, Rae-Hong Jung, and Minkyu Choi. 2008. "Wastewater Treatment Plants (WWTPs) as a Source of Sediment Contamination by Toxic Organic Pollutants and Fecal Sterols in a Semi-Enclosed Bay in Korea." *Chemosphere* 73 (6): 880–89. https://doi.org/10.1016/j.chemosphere.2008.07.038.

Morelissen, Robin, Theo van der Kaaij, and Tobias Bleninger. 2013. "Dynamic Coupling of near Field and Far Field Models for Simulating Effluent Discharges." *Water Science and Technology* 67 (10): 2210–20. https://doi.org/10.2166/wst.2013.081.

Mrša Haber, Iva, Tarzan Legović, Lado Kranjčević, and Marijan Cukrov. 2020. "Simulation of Pollutants Spreading from a Sewage Outfall in the Rijeka Bay." *Mediterranean Marine Science* 21 (1): 116–28. https://doi.org/10.12681/mms.20467.

Murakami, Mayumi, Yukio Oonishi, and Hideaki Kunishi. 1985. "A Numerical Simulation of the Distribution of Water Temperature and Salinity in the Seto Inland Sea." *Journal of the Oceanographical Society of Japan* 41 (4): 213–24. https://doi.org/10.1007/BF02109271.

Neves, M. J., and H. J. S. Fernando. 1995. "Sedimentation of Particles from Jets Discharged by Ocean Outfalls: A Theoretical and Laboratory Study." *Water Science and Technology* 32 (2): 133–39. https://doi.org/10.2166/wst.1995.0088.

Neves, Ramiro. 2006. "Modelling Applied to Waste Disposal Systems. Application of MOHID for Simulating Trophic Activity in the Tagus and for Assessing the Impact of Costa Do Estoril Submarine Outfall." In *Submarine Outfalls: Design, Compliance and Environmental*

Monitoring, 147–69. São Paulo, Brazil: Secretaria do Meio Ambiente do Estado de São Paulo.
Ormondt, Maarten van, Kees Nederhoff, and Ap van Dongeren. 2020. "Delft Dashboard: A Quick Set-up Tool for Hydrodynamic Models." *Journal of Hydroinformatics* 22 (3): 510–27. https://doi.org/10.2166/hydro.2020.092.
Ostoich, Marco, Michol Ghezzo, Georg Umgiesser, Mirco Zambon, Loris Tomiato, Federico Ingegneri, and Giuseppe Mezzadri. 2018. "Modelling as Decision Support for the Localisation of Submarine Urban Wastewater Outfall: Venice Lagoon (Italy) as a Case Study." *Environmental Science and Pollution Research* 25 (34): 34306–18. https://doi.org/10.1007/s11356-018-3316-0.
Pearson, Stuart G., Bram C. van Prooijen, Jack Poleykett, Matthew Wright, Kevin Black, and Zheng Bing Wang. 2021. "Tracking Fluorescent and Ferrimagnetic Sediment Tracers on an Energetic Ebb-Tidal Delta to Monitor Grain Size-Selective Dispersal." *Ocean & Coastal Management* 212:105835. https://doi.org/10.1016/j.ocecoaman.2021.105835.
Pianca, Cássia, Piero Luigi F. Mazzini, and Eduardo Siegle. 2010. "Brazilian Offshore Wave Climate Based on NWW3 Reanalysis." *Brazilian Journal of Oceanography* 58 (1): 53–70. https://doi.org/10.1590/s1679-87592010000100006.
Pokavanich, Tanuspong, Kazuo Nadaoka, and Ariel C. Blanco. 2008. "Comprehensive Circulation and Water Quality Investigation of the Coastal Lagoon: Puerto Galera, the Philippines." In *Proceedings of the 8th International Conference on Hydro-Science and Engineering*, edited by Sam S. Y. Wang, 1–10. Nagoya, Japan: Nagoya Hydraulic Research Institute for River Basin Management. https://hdl.handle.net/20.500.11970/110193.
Pontius Jr., Robert Gilmore. 2022. *Metrics That Make a Difference*. Advances in Geographic Information Science. Springer.
Pritchard, Daniel, Graham Savidge, and Björn Elsäßer. 2013. "Coupled Hydrodynamic and Wastewater Plume Models of Belfast Lough, Northern Ireland: A Predictive Tool for Future Ecological Studies." *Marine Pollution Bulletin* 77 (1): 290–99. https://doi.org/10.1016/j.marpolbul.2013.09.046.
Reed, Sarah, Marlon Clark, Richard Thompson, and Kevin A. Hughes. 2018. "Microplastics in Marine Sediments near Rothera Research Station, Antarctica." *Marine Pollution Bulletin* 133:460–63. https://doi.org/10.1016/j.marpolbul.2018.05.068.
Ris, R. C., L. H. Holthuijsen, and N. Booij. 1999. "A Third-Generation Wave Model for Coastal Regions: 2. Verification." *Journal of Geophysical Research: Oceans* 104 (C4): 7667–81. https://doi.org/10.1029/1998jc900123.
Roberts, Philip J. W. 1991. "Ocean Outfalls." *Critical Reviews in Environmental Control* 20 (5–6): 311–39. https://doi.org/10.1080/10643389109388404.
Roberts, Philip J. W., Henry J. Salas, Fred M. Reiff, Menahem Libhaber, Alejandro Labbe, and James C. Thomson. 2010. *Marine Wastewater Outfalls and Treatment Systems*. IWA Publishing. https://doi.org/10.2166/9781780401669.
Roberts, Philip J. W., and Beatriz Villegas. 2017. "Modeling and Design of the Buenos Aires Outfalls." *Journal of Hydraulic Engineering* 143 (2): 05016007. https://doi.org/10.1061/(ASCE)HY.1943-7900.0001244.
Ruiz, Matheus S., Joseph Harari, Renan B. Ribeiro, and Alexandra F.P. Sampaio. 2021. "Numerical Modelling of Storm Tides in the Estuarine System of Santos, São Vicente and Bertioga (SP, Brazil)." *Regional Studies in Marine Science* 44:101791. https://doi.org/10.1016/j.rsma.2021.101791.
Rusu, Liliana. 2022. "The near Future Expected Wave Power in the Coastal Environment of the Iberian Peninsula." *Renewable Energy* 195:657–69. https://doi.org/10.1016/j.renene.2022.06.047.
Sabesp. 2023. "Revisão e Atualização Do Plano Diretor de Abastecimento de Água e a Elaboração Do Plano Diretor de Esgotamento Sanitário Da Região Metropolitana Da Baixada Santista PDAAES–RMBS." Companhia de Saneamento Básico do Estado de São Paulo (Sabesp).

Saha, Suranjana, Shrinivas Moorthi, Xingren Wu, Jiande Wang, Sudhir Nadiga, Patrick Tripp, David Behringer, et al. 2014. “The NCEP Climate Forecast System Version 2.” *Journal of Climate* 27 (6): 2185–2208. https://doi.org/10.1175/JCLI-D-12-00823.1.

Santos, Dayana M. dos, Lucas Buruaem, Renato M. Gonçalves, Mike Williams, Denis M. S. Abessa, Rai Kookana, and Mary Rosa R. de Marchi. 2018. “Multiresidue Determination and Predicted Risk Assessment of Contaminants of Emerging Concern in Marine Sediments from the Vicinities of Submarine Sewage Outfalls.” *Marine Pollution Bulletin* 129 (1): 299–307. https://doi.org/10.1016/j.marpolbul.2018.02.048.

Schettini, Carlos A. F., Eliane C. Truccolo, José A. D. Mattos, and Daniel C. D. A. Benevides. 2019. “Tides and Sea Level Variability Decomposition in the Port of Santos Waterway.” *Brazilian Journal of Oceanography* 67. https://doi.org/10.1590/s1679-87592019026506707.

Smith, Grant A., Mark Hemer, Diana Greenslade, Claire Trenham, Stefan Zieger, and Tom Durrant. 2021. “Global Wave Hindcast with Australian and Pacific Island Focus: From Past to Present.” *Geoscience Data Journal* 8 (1): 24–33. https://doi.org/10.1002/gdj3.104.

Soto-Jiménez, M., F. Páez-Osuna, and F. Morales-Hernández. 2001. “Selected Trace Metals in Oysters (Crassostrea Iridescens) and Sediments from the Discharge Zone of the Submarine Sewage Outfall in Mazatlán Bay (Southeast Gulf of California): Chemical Fractions and Bioaccumulation Factors.” *Environmental Pollution* 114 (3): 357–70. https://doi.org/10.1016/S0269-7491(00)00239-6.

Soulsby RL, Hamm L, Klopman G, Myrhaug D, Simons RR, Thomas GP. 1993. Wave-current interaction within and outside the bottom boundary layer. Coastal Engineering. 21(1-3):41–69. doi:10.1016/0378-3839(93)90045-a.

Soulsby, R. L., and J. D. Humphery. 1990. “Field Observations of Wave-Current Interaction at the Sea Bed.” In *Water Wave Kinematics*, edited by A. Tørum and O. T. Gudmestad, 178:413–28. NATO ASI Series. Dordrecht, Netherlands: Springer. https://doi.org/10.1007/978-94-009-0531-3_25.

Sousa, E. C. P. M., Letícia Pires Zaroni, Marcia Regina Gasparro, and Camilo Dias Seabra Pereira. 2014. “Review of Ecotoxicological Studies of the Marine and Estuarine Environments of the Baixada Santista (São Paulo, Brazil).” *Brazilian Journal of Oceanography* 62 (2): 133–47. https://doi.org/10.1590/S1679-87592014063006202.

Stech, José L., and João A. Lorenzzetti. 1992. “The Response of the South Brazil Bight to the Passage of Wintertime Cold Fronts.” *Journal of Geophysical Research: Oceans* 97 (C6): 9507–20. https://doi.org/10.1029/92JC00486.

Stein, Luiza Paschoal, and Eduardo Siegle. 2019. “Santos Beach Morphodynamics under High-Energy Conditions.” *Revista Brasileira de Geomorfologia* 20 (3). https://doi.org/10.20502/rbg.v20i3.1419.

Stopa, Justin E. 2018. “Wind Forcing Calibration and Wave Hindcast Comparison Using Multiple Reanalysis and Merged Satellite Wind Datasets.” *Ocean Modelling* 127:55–69. https://doi.org/10.1016/j.ocemod.2018.04.008.

Suárez, J., and J. Puertas. 2005. “Determination of COD, BOD, and Suspended Solids Loads during Combined Sewer Overflow (CSO) Events in Some Combined Catchments in Spain.” *Ecological Engineering* 24 (3): 199–217. https://doi.org/10.1016/j.ecoleng.2004.11.005.

Tate, Peter M., C. J. Holden, and D. J. Tate. 2019. “Influence of Plume Advection and Particle Settling on Wastewater Dispersion and Distribution.” *Marine Pollution Bulletin* 145:678–90. https://doi.org/10.1016/j.marpolbul.2019.05.059.

Tate, Peter M., Salvatore Scaturro, and Bruce Cathers. 2016. “Marine Outfalls.” In *Springer Handbook of Ocean Engineering*, 711–40. Cham, Switzerland: Springer International Publishing. https://doi.org/10.1007/978-3-319-16649-0_32.

Terfous, Abdelali, Samia Chiban, and Abdellah Ghenaim. 2016. “Modeling Sediment Deposition from Marine Outfall Jets.” *Environmental Technology* 37 (15): 1865–74. https://doi.org/10.1080/09593330.2015.1135988.

Tozer, B., D. T. Sandwell, W. H. F. Smith, C. Olson, J. R. Beale, and P. Wessel. 2019. “Global Bathymetry and Topography at 15 Arc Sec: SRTM15+.” *Earth and Space Science* 6 (10): 1847–64. https://doi.org/10.1029/2019EA000658.

Uchiyama, Yusuke, Eileen Y. Idica, James C. McWilliams, and Keith D. Stolzenbach. 2014. “Wastewater Effluent Dispersal in Southern California Bays.” *Continental Shelf Research* 76:36–52. https://doi.org/10.1016/j.csr.2014.01.002.

Vacchi, Francine I., Amanda dos Santos, Mariana C. Artal, Gabriel R. Magalhães, Josiane A. de Souza Vendemiatti, and Gisela de Aragão Umbuzeiro. 2019. “Parhyale Hawaiensis as a Promising Alternative Organism for Monitoring Acute Toxicity of Sediments under the Influence of Submarine Outfalls.” *Marine Pollution Bulletin* 149:110658. https://doi.org/10.1016/j.marpolbul.2019.110658.

Veríssimo, F., and F. Martins. 2016. “Impact of Albufeira Bay (Portugal) Outfall Plumes in Bathing Water Quality, a Modelling Approach.” In *Proceedings of the International Symposium on Outfall Systems, 2016*, 1–10. Ottawa, Canada: IAHR. http://www.iahr.org.cn/library/infor?pid=9188.

Violante-Carvalho, Nelson, Carlos Eduardo Parente, Ian S. Robinson, and Luis Manoel P. Nunes. 2001. “On the Growth of Wind-Generated Waves in a Swell-Dominated Region in the South Atlantic.” *Journal of Offshore Mechanics and Arctic Engineering* 124 (1): 14–21. https://doi.org/10.1115/1.1423636.

Vledder, G. van, Marcel Zijlema, and L. H. Holthuijsen. 2011. “Revisiting the JONSWAP Bottom Friction Formulation.” In *Proceedings of 32nd International Conference on Coastal Engineering, Shanghai, China, 2010*, edited by Jane McKee Smith and Patrick Lynett, 455–62. https://doi.org/10.9753/icce.v32.waves.41.

Wasserman, J. C., A. A. P. Freitas-Pinto, and D. Amouroux. 2000. “Mercury Concentrations in Sediment Profiles of a Degraded Tropical Coastal Environment.” *Environmental Technology* 21 (3): 297–305. https://doi.org/10.1080/09593332108618117.

Wolf, Judith. 2009. “Coastal Flooding: Impacts of Coupled Wave–Surge–Tide Models.” *Natural Hazards* 49 (2): 241–60. https://doi.org/10.1007/s11069-008-9316-5.

Wu, Yicun, Libe Washburn, and Burton H. Jones. 1991. “Mixing and Dispersion Processes in the Vicinity of an Ocean Outfall System in Southern California.” In *Coastal Zone ’91: Proceedings of the Seventh Symposium on Coastal and Ocean Management*, edited by Orville T. Magoon, Hugh Converse, Virginia Tippie, L. Thomas Tobin, and Delores Clark, 124–34. Long Beach, CA: American Society of Civil Engineers. https://cedb.asce.org/CEDBsearch/record.jsp?dockey=0071341.

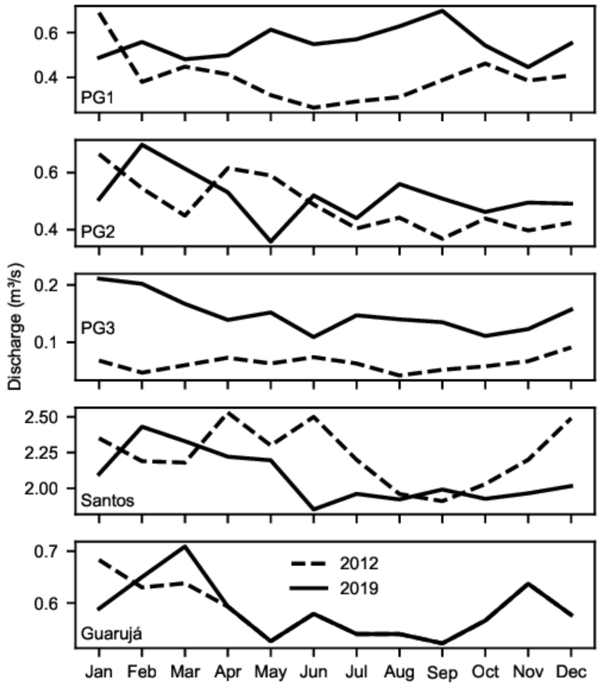

Figure A1: Average monthly discharges of the outfalls.

Table A1: Mean annual flows (m^3/s) for freshwater point discharges.

Label	2012	2019
PT-01	0.25	0.25
PT-02	0.50	0.52
PT-03	0.62	0.65
PT-04	0.62	0.65
PT-05	0.65	0.68
PT-06	0.37	0.39
PT-07	0.46	0.48
PT-08	0.41	0.40
PT-09	0.17	0.17
PT-10	0.53	0.51
PT-11	0.63	0.61
PT-12	1.31	1.27
PT-13	0.40	0.42
PT-14	1.98	2.07
PT-15	2.83	2.95
PT-16	9.71	10.15
PT-17	9.09	9.49
PT-18	9.36	9.08
PT-19	4.13	4.01
PT-20	1.57	1.53
PT-21	0.15	0.15
PT-22	1.63	1.58
PT-23	1.65	1.60
PT-24	0.80	0.78
PT-25	1.74	1.69
PT-26	1.33	1.29
PT-27	25.26	24.52

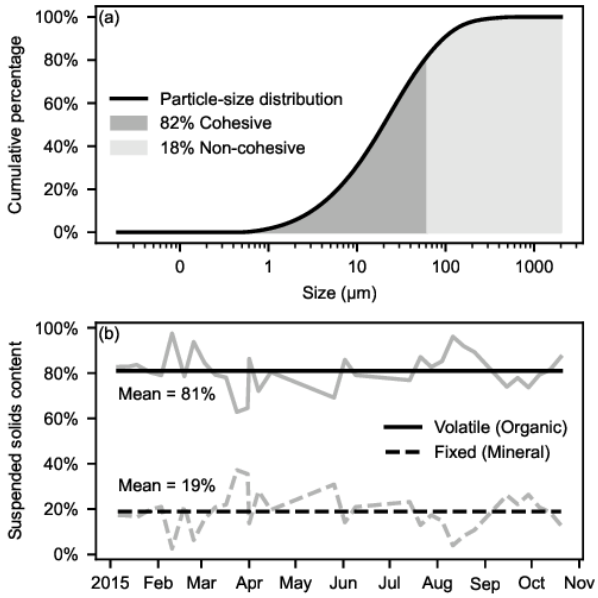

Figure A2: Granulometry (a) and composition (b) of effluent solids from the Santos treatment plant (Consórcio Partner/TetraTech 2017).

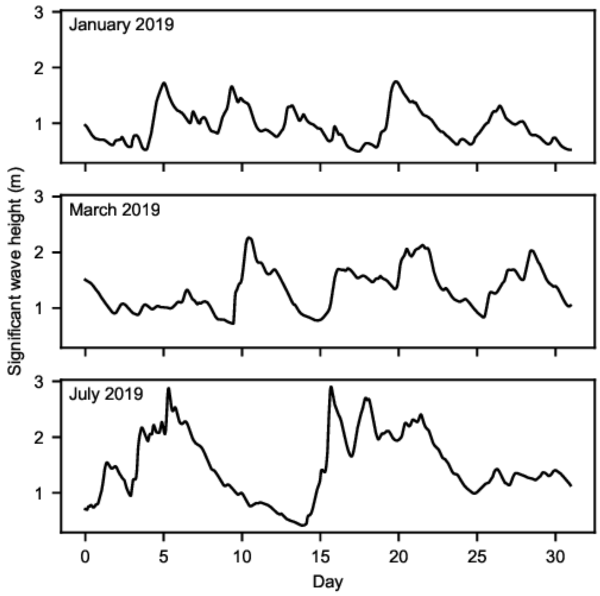

Figure A3: Time series of significant wave height from the western CAWCR node (24.4°S, 46.4°W).

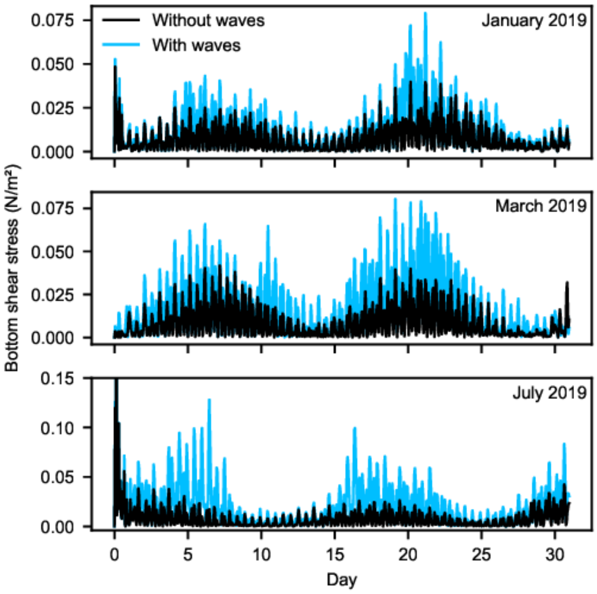

Figure A4: Modeled bed shear stress in the vicinity of the Santos outfall diffuser.